

การกักเก็บฟลูออไรด์ในเมทริกซ์แคลเซียม

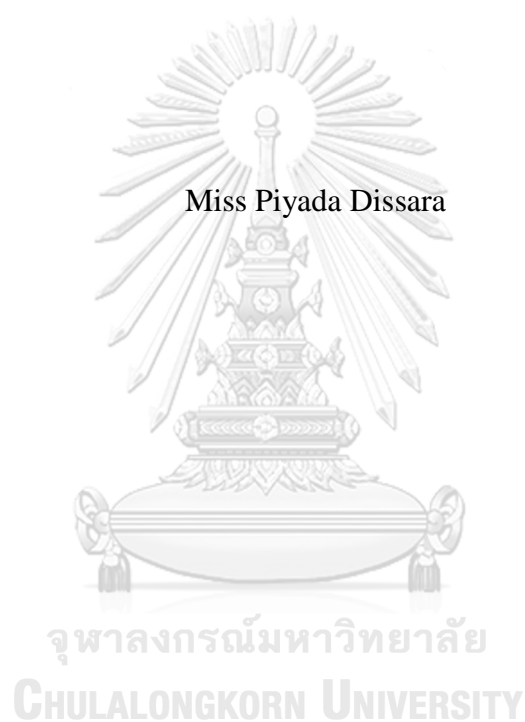


บทคัดย่อและแฟ้มข้อมูลฉบับเต็มของวิทยานิพนธ์ตั้งแต่ปีการศึกษา 2554 ที่ให้บริการในคลังปัญญาจุฬาฯ (CUIR)
เป็นแฟ้มข้อมูลของนิสิตเจ้าของวิทยานิพนธ์ ที่ส่งผ่านทางบัณฑิตวิทยาลัย

The abstract and full text of theses from the academic year 2011 in Chulalongkorn University Intellectual Repository (CUIR)
are the thesis authors' files submitted through the University Graduate School.

วิทยานิพนธ์นี้เป็นส่วนหนึ่งของการศึกษาตามหลักสูตรปริญญาวิทยาศาสตรมหาบัณฑิต
สาขาวิชาเคมี ภาควิชาเคมี
คณะวิทยาศาสตร์ จุฬาลงกรณ์มหาวิทยาลัย
ปีการศึกษา 2560
ลิขสิทธิ์ของจุฬาลงกรณ์มหาวิทยาลัย

FLUORIDE ENCAPSULATION IN CALCIUM MATRIX



A Thesis Submitted in Partial Fulfillment of the Requirements
for the Degree of Master of Science Program in Chemistry
Department of Chemistry
Faculty of Science
Chulalongkorn University
Academic Year 2017
Copyright of Chulalongkorn University

ปิยะญา ดิสสระ : การกักเก็บฟลูออไรด์ในเมทริกซ์แคลเซียม (FLUORIDE ENCAPSULATION IN CALCIUM MATRIX) อ.ที่ปรึกษาวิทยานิพนธ์หลัก: ผศ. ดร.พร้อมพงศ์ เพียรพินิจธรรม, 65 หน้า.

ฟลูออไรด์เป็นส่วนประกอบที่สำคัญในยาสีฟัน ช่วยป้องกันฟันผุโดยเกิดปฏิกิริยากับไฮดรอกซีอะพาไทต์ $[Ca_{10}(PO)_4(OH)_2]$ ที่อยู่ในสารเคลือบฟันเกิดเป็นฟลูออโรอะพาไทต์ $[Ca_{10}(PO)_4(F)_2]$ ซึ่งละลายน้ำได้ยาก อย่างไรก็ตามฟลูออไรด์เกิดปฏิกิริยากับแคลเซียมสปีชีส์ในยาสีฟันได้ง่าย ส่งผลให้ฟลูออไรด์ไม่สามารถเกิดปฏิกิริยากับสารเคลือบฟันได้ งานวิจัยนี้มุ่งเน้นที่จะขึ้นรูปเม็ดพอลิเมอร์เพื่อใช้ในการรักษาสมบัติของฟลูออไรด์ด้วยวิธีการเอ็กซ์ทรูชันอย่างง่าย สำหรับกระบวนการขึ้นรูปเม็ดพอลิเมอร์มีขั้นตอนดังนี้ หยดสารละลายน้ำของฟลูออไรด์ลงในสารละลายเซลล์ที่ละลายในเอทานอล เม็ดพอลิเมอร์จะเกิดขึ้นด้วยสมบัติการไม่ละลายน้ำของเซลล์เล็ก หลังจากนั้นเม็ดพอลิเมอร์ถูกนำไปแช่ในน้ำเพื่อทำให้เม็ดพอลิเมอร์แข็งตัวซึ่งเกิดจากการแพร่ของเอทานอลในผนังของเม็ดพอลิเมอร์ไปสู่ชั้นน้ำ กลไกในการเกิดเม็ดพอลิเมอร์ถูกศึกษาด้วยอินฟราเรดสเปกโทรสโกปี การขึ้นรูปเม็ดพอลิเมอร์ถูกปรับเงื่อนไขให้เหมาะสมโดยปรับเปลี่ยนความเข้มข้นของสารละลายเซลล์ เวลาในการละลายเซลล์ในเอทานอล เวลาในการเกิด เม็ดพอลิเมอร์ และเวลาในการแข็งตัวของเม็ดพอลิเมอร์ในน้ำ จากการทดลองพบว่า เม็ดพอลิเมอร์ที่ได้มีขนาด 2.59 ± 0.33 มิลลิเมตร ฟลูออไรด์ถูกปลดปล่อยออกจากเม็ดพอลิเมอร์ทั้งหมดหลังจากแช่ในน้ำเป็นเวลา 14 วัน แต่เมื่อแช่เม็ดพอลิเมอร์ในสารละลายแคลเซียมคลอไรด์ที่มีความเข้มข้น 5 % พบว่าเม็ดพอลิเมอร์สามารถกักเก็บฟลูออไรด์ได้ 71.03 ± 4.18 % เป็นเวลาอย่างน้อย 3 เดือน เนื่องจากแคลเซียมฟลูออไรด์สามารถปิดช่องการปลดปล่อยฟลูออไรด์บนผิวของเม็ดพอลิเมอร์ได้

CHULALONGKORN UNIVERSITY

ภาควิชา เคมี
สาขาวิชา เคมี
ปีการศึกษา 2560

ลายมือชื่อนิสิต

ลายมือชื่อ อ.ที่ปรึกษาหลัก

5871993023 : MAJOR CHEMISTRY

KEYWORDS: FLUORIDE ION / ENCAPSULATION / SHELLAC

PIYADA DISSARA: FLUORIDE ENCAPSULATION IN CALCIUM MATRIX. ADVISOR: ASST. PROF.PROMPONG PIENPINIJTHAM, Ph.D., 65 pp.

Fluoride ion (F^-) is an important ingredient in a toothpaste. It protects caries by reacting with hydroxyapatite [$Ca_{10}(PO)_4(OH)_2$] in tooth enamel to form insoluble fluorapatite [$Ca_{10}(PO)_4(F)_2$]. Unfortunately, F^- also easily interacts with calcium species in a toothpaste, and then it is deactivated. In this work, we focus on the encapsulation of F^- in a shellac bead by using a simple extrusion method. To construct shellac beads, an aqueous solution of F^- is injected into an ethanolic solution of shellac. The shellac beads are formed due to insolubility of shellac in water. Then, the beads are transferred into DI water for hardening a bead wall *via* a diffusion of ethanol in the bead wall to an aqueous phase. The bead formation mechanism is investigated using infrared spectroscopy. The process is also optimized by varying shellac concentration, shellac-dissolution time, bead-formation time, and bead-hardening time. The average size of F^- -encapsulated shellac beads is 2.59 ± 0.33 mm. Active F^- is completely released from shellac beads after immersed in DI water for 14 days. Surprisingly, after immersed in 5 % $CaCl_2$, the beads can encapsulate the active F^- for, at least, 3 months with the percentage of active F^- remaining in the beads of 71.03 ± 4.18 %. It is because CaF_2 can block releasing channels of active F^- on the bead surface.

Department: Chemistry

Student's Signature

Field of Study: Chemistry

Advisor's Signature

Academic Year: 2017

ACKNOWLEDGEMENTS

I would like to express my sincere gratitude for my thesis, to Assistant Professor Dr. Prompong Pienpinijtham (my thesis advisor), Assistant Professor Dr. Kanet Wongravee, and Professor Dr. Sanong Ekgasit, for their useful guidances, kind suggestions, financial supports, and their training on the initiating of scientific ideas and solving problems during my research.

I would like to thank Associate Professor Dr. Vudhichai Parasuk, Associate Professor Dr. Sumrit Wacharasindhu, Dr. Sakulsuk Unarunotai, and Associate Professor Dr. Pimthong Thongnopkun for serving as chairman and members of thesis committees for useful suggestions, valuable discussions, and helpful comments.

I would like to thank all members of Sensor Research Unit (SRU), Department of Chemistry, Faculty of Science for exceptional friendship and encouragement.

Most importantly, I am profoundly grateful to my beloved family for all their loves, understanding to my decisions, encouragement during the entire period of my study.

CONTENTS

	Page
THAI ABSTRACT	iv
ENGLISH ABSTRACT.....	v
ACKNOWLEDGEMENTS	vi
CONTENTS.....	vii
LIST OF FIGURES	ix
LIST OF ABBREVIATION AND SYMBOLS	xiii
CHAPTER I INTRODUCTION.....	1
1.1 Introduction.....	1
1.2 Objective.....	5
1.3 Scopes of research	5
CHAPTER II THEORETICAL BACKGROUND.....	6
2.1 Encapsulation process.....	6
2.1.1 Spray drying	6
2.1.2 Spray chilling and spray cooling	7
2.1.3 Freeze drying.....	8
2.1.4 Air suspension coating	9
2.1.5 Extrusion	11
2.1.6 Coacervation.....	12
2.2 Materials for encapsulation.....	13
2.3 Encapsulation of F ⁻ in gelatin and ethylcellulose microparticles	14
CHAPTER III METHODOLOGY	16
3.1 Chemicals.....	16
3.2 Preparation of shellac bead	16
3.3 Characterizations	17
3.3.1 Size and wall thickness of shellac beads	17
3.3.2 Morphology and chemical composition	18
3.3.2.1 Scanning electron microscopy (SEM).....	18
3.3.2.2 Energy-dispersive X-ray spectroscopy (EDS).....	18

	Page
3.3.2.3 Fourier-transform infrared (FT-IR) spectroscopy	18
3.3.3 Crystallinity	19
3.3.4 Efficiency to store F ⁻	19
CHAPTER IV RESULTS AND DISCUSSION.....	20
4.1 Size and wall thickness of shellac beads	20
4.2 The formation mechanism of shellac beads.....	21
4.3 Optimization for the preparation of shellac beads	26
4.3.1 Effect of shellac concentration.....	27
4.3.2 Effect of shellac-dissolution time.....	29
4.3.3 Effect of bead-formation time	33
4.3.4 Effect of bead-hardening time.....	35
4.4 F ⁻ encapsulation in 5 % CaCl ₂ solution	40
4.5 Morphology of shellac beads in 5 % CaCl ₂	43
4.6 The proposed mechanism of CaF ₂ formation on the bead surface	46
CHAPTER V CONCLUSIONS	49
5.1 Conclusions.....	49
5.2 Suggestions	50
REFERENCES	51
VITA.....	65

LIST OF FIGURES

Figure	Page
1.1	4
2.1	7
2.2	11
2.3	12
3.1	17
4.1	21
4.2	23

Figure	Page
4.3	The formation of shellac film by an evaporation of ethanol from shellac solution..... 24
4.4	IR spectra of shellac before dissolved in ethanol, shellac film, shellac beads..... 25
4.5	The formation of shellac beads by a diffusion of ethanol from shellac solution to aqueous phases..... 26
4.6	Percentages of active F ⁻ remaining in shellac beads prepared by using different shellac concentrations (60–80 %) after immersed in DI water (1–7 days)..... 28
4.7	SEM images of bead surfaces prepared by using ethanolic solutions of (A) 70 and (B) 80 % shellac..... 29
4.8	Percentages of active F ⁻ remaining in shellac beads prepared by using various shellac-dissolution times after immersed in DI water (1–7 days)..... 31
4.9	DSC thermograms of shellac before dissolved in ethanol and shellac beads prepared by using shellac-dissolution times of 1 and 5 days..... 33

Figure	Page
4.10 Percentages of active F^- remaining in shellac beads prepared by using various bead-formation times after immersed in DI water (1–7 days).....	35
4.11 Percentages of active F^- remaining in shellac beads prepared by using various bead-hardening times after immersed in DI water (1–7 days).....	37
4.12 SEM images of bead surfaces (A) before and (B) after immersed in DI water for 7 days.....	39
4.13 IR spectra of bead surfaces (A) before and (B) after immersed in DI water for 7 days.....	40
4.14 Percentages of active F^- remaining in shellac beads after immersed in DI water and 5 % $CaCl_2$ for 1–14 days.....	41
4.15 Percentages of active F^- remaining in shellac beads after immersed in 5 % $CaCl_2$ for 1–90 days.....	42
4.16 SEM images of bead surfaces (A) before and (B) after immersed in 5 % $CaCl_2$ for 7 days.....	44

Figure	Page
4.17 (A) SEM image and elemental maps of (B) carbon, (C) oxygen, (D) fluoride, and (E) calcium collected from the surface of shellac bead after immersed in 5 % CaCl ₂ for 7 days, (F) EDS spectrum collected from the (×) position in Figure 4.17A.....	45
4.18 (A) SEM image and elemental maps of (B) carbon, (C) oxygen, (D) fluoride, and (E) calcium collected from the shellac bead wall after immersed in 5 % CaCl ₂ for 7 days...	47
4.19 The proposed mechanism of the CaF ₂ formation on the bead surface.....	48

LIST OF ABBREVIATION AND SYMBOLS

F^-	: fluoride ion
HF	: hydrofluoric acid
$Ca_{10}(PO)_4(OH)_2$: hydroxyapatite
$Ca_{10}(PO)_4(F)_2$: fluorapatite
OH^-	: hydroxide ion
$CaCl_2$: calcium chloride
MFP	: monofluorophosphate
NaF	: sodium fluoride
K_{sp}	: solubility product constant
FT-IR	: Fourier Transform Infrared Spectroscopy
%w/v	: weight by volume percent
g	: gram
mL	: milliliter
μL	: microliter
mm	: millimeter
ppm	: part per million
cm^{-1}	: reciprocal centimeters
$^{\circ} C$: degree Celsius

DI water : deionized water

Ca^{2+} : calcium ion

CaF_2 : calcium chloride



CHAPTER I

INTRODUCTION

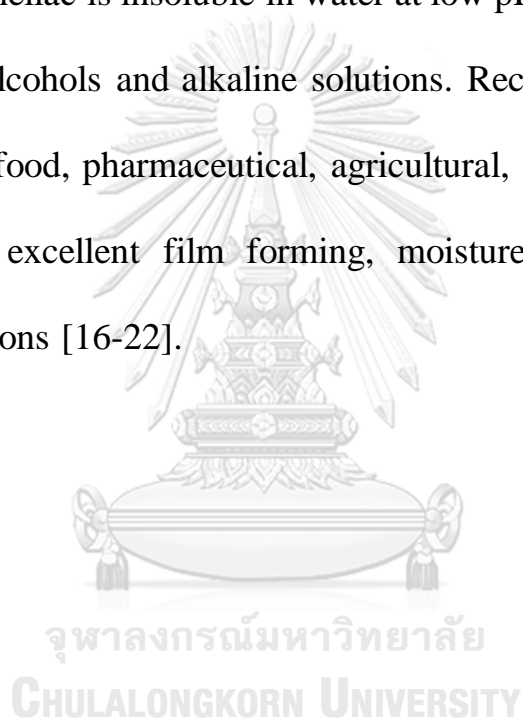
1.1 Introduction

Fluoride ion (F^-) is a crucial ingredient in a toothpaste because it can protect tooth decay. The mechanism of F^- for protecting dental caries comprises of inhibiting bacterial enzymes, inhibiting demineralization, and enhancing remineralization [1]. Some researchers found that F^- cannot pass through a cell wall of bacteria but it is partly converted to hydrofluoric acid (HF), which can inhibit bacterial enzymes in acidic conditions produced by bacteria themselves [2-4]. The process of demineralization simultaneously occurs because bacteria produce acids such as lactic, acetic, propionic, and formic acids by metabolizing fermentable carbohydrates. These acids can dissolve calcium phosphate minerals in a tooth enamel [5-6]. F^- enhances remineralization by reacting with hydroxyapatite $[Ca_{10}(PO)_4(OH)_2]$ in tooth enamel to form insoluble fluorapatite $[Ca_{10}(PO)_4(F)_2]$. For this chemical reaction, the hydroxide ion (OH^-) in hydroxyapatite is completely replaced by F^- [1, 5, 7]. Fluorapatite is highly resistant to acidic dissolution because the solubility constant of fluorapatite ($K_{sp} = 3.2 \times 10^{-61}$) is lower than hydroxyapatite ($K_{sp} = 5.0 \times 10^{-55}$) [8].

Unfortunately, F^- can also interact with calcium species in the toothpaste (e.g., calcium phosphate and calcium carbonate) causing F^- to be deactivated [9]. Therefore, to store F^- and calcium species together in the toothpaste is very challenging.

An encapsulation process is defined as a process to entrap one material within another material by forming a small bead. The entrapped material is called core material, active agent, or internal phase while the entrapping material is called coating, membrane shell, wall material, or external phase. This process has been continuously developed until now. There are several processes that are used to encapsulate active ingredients such as spray drying, spray cooling, freeze drying, fluidized bed coating, extrusion, and coacervation. The encapsulation process is widely used in various applications, such as food, medical, pharmaceutical, cosmetic, chemical, agricultural, and printing industries. The advantage of this process is to protect active ingredients (e.g., vitamins, minerals, colorants, enzymes, and agro-chemicals) from pH, moisture, light, or oxygen. In addition, this technique can enhance shelf-life and stability of some active ingredients until they are required to be released [10-15]. Generally, polymers, such as alginate, gelatin, chitosan, carrageenan, and shellac, are used as a wall material due to their nontoxicity, biodegradability, and biocompatibility.

Shellac is a natural polymer produced by lac insect, *Kerria lacca*, which parasitically grows on host trees in China, India, and Thailand. Shellac has a complicated chemical structure which contains hard and soft resins of polyester and single ester (see chemical structure of shellac in Figure 1.1). The main acid component consists of aleuritic acid and terpenic acid. Shellac is insoluble in water at low pH or in acidic solutions, but soluble in alcohols and alkaline solutions. Recently, shellac has been widely used in food, pharmaceutical, agricultural, and painting industries because of an excellent film forming, moisture protecting, and acid resisting conditions [16-22].



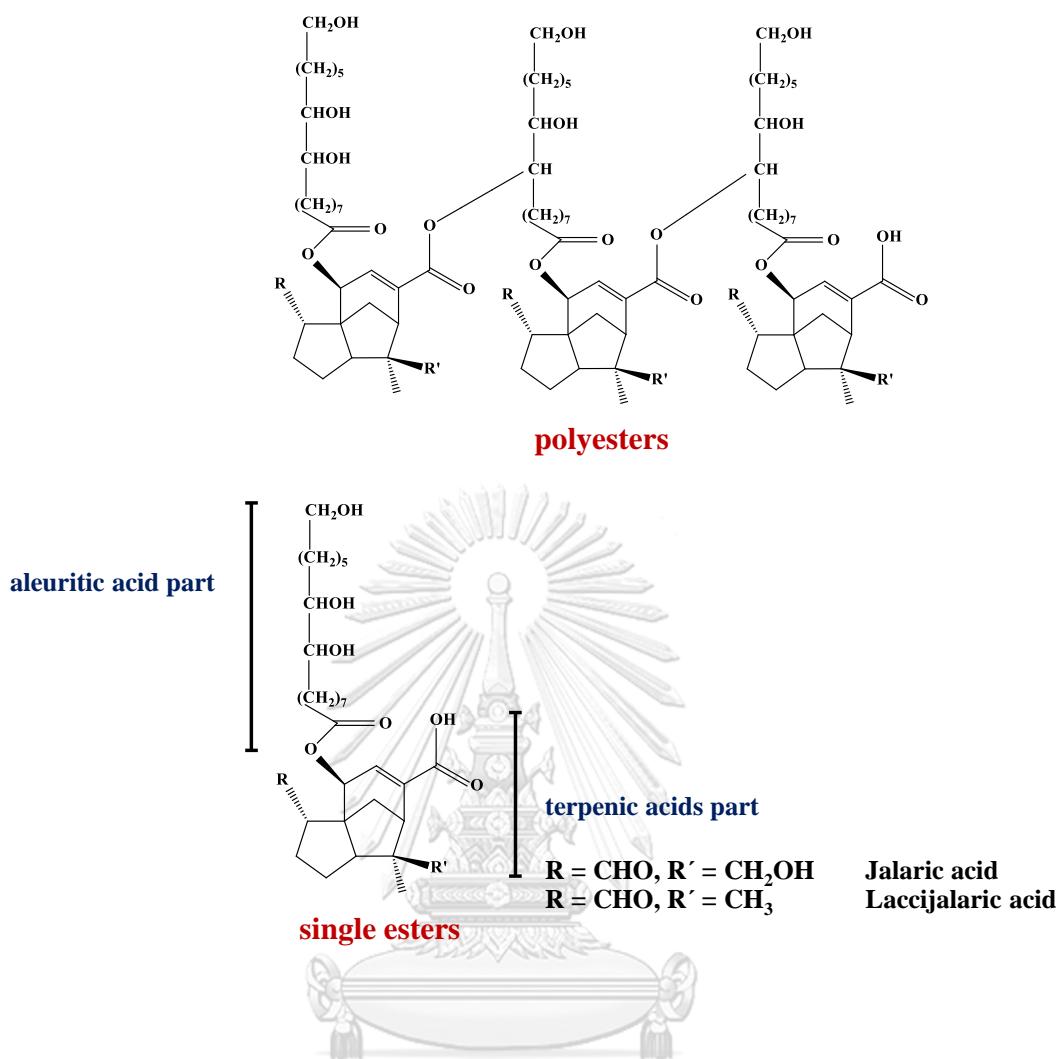


Figure 1.1 Chemical structure of shellac.

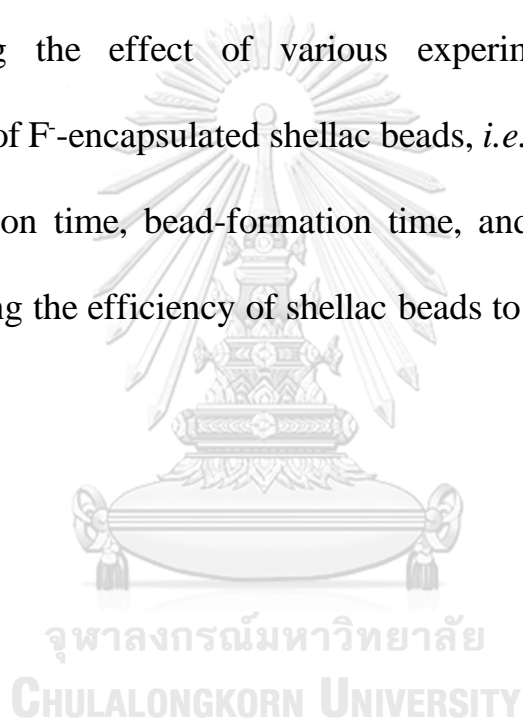
In this work, we propose a simple extrusion method to fabricate polymer beads from shellac for encapsulating F⁻, and study various experimental parameters to entrap F⁻ in polymer beads for a long shelf-life time. The efficiency of shellac beads to store F⁻ in calcium matrix is also investigated for a use in a toothpaste application.

1.2 Objective

To fabricate the F⁻-encapsulated shellac beads which can maintain properties of F⁻ in a calcium matrix.

1.3 Scopes of research

Studying the effect of various experimental parameters on the preparation of F⁻-encapsulated shellac beads, *i.e.*, shellac concentration, shellac-dissolution time, bead-formation time, and bead-hardening time, and then studying the efficiency of shellac beads to store F⁻ in a 5 % CaCl₂ solution.



CHAPTER II

THEORETICAL BACKGROUND

2.1 Encapsulation process

Generally, the encapsulation process has various processes that were used to encapsulate active ingredients. Here, common encapsulation processes are introduced.

2.1.1 Spray drying

Spray drying is the oldest process that was used to encapsulate active ingredients. It is commonly used in a food industry because this process can encapsulate active ingredients into dry ingredients. The advantages of this process include shelf-life extension, good stability of active ingredient, good preservation of volatile, low process cost, and large-scale production of food industry. However, the limitation of this process is that it cannot encapsulate some ingredients with low boiling points because the active ingredients may be coated on a bead surface causing a deactivation during a spray drying process. Properties of good wall materials for spray drying are good emulsifying agent, low viscosity, and low hygroscopicity.

The process of a spray drying begins with a dissolution of an active ingredient in an aqueous solution of wall material. All components are atomized into heated air for rapid evaporation of water. Droplets are mixed with hot air in a drying chamber causing the encapsulation of active ingredients in the wall material. The resulting powder particles are separated from drying air at lower temperature [10, 13, 23-25], as shown in Figure 2.1.

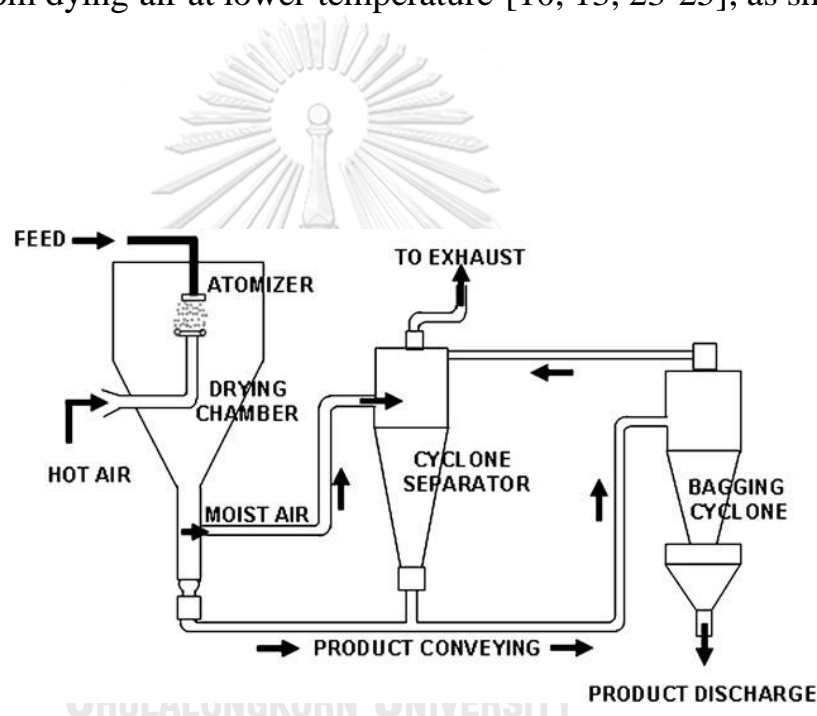


Figure 2.1 Schematic drawing of the spray drying process.

2.1.2 Spray chilling and spray cooling

Spray chilling and spray cooling are the least expensive technology to encapsulate active ingredients. Firstly, the active ingredients are mixed

with fat or oil, and then the solution is transferred into a cold air spray dryer. Finally, this method produces free flowing powder that is the active ingredients encapsulated in fat or oil. Generally, those processes are quite similar to spray drying, but there is no water evaporated from wall material in the drying chamber. Moreover, the wall materials in this process are hydrophobic materials, such as hydrogenated vegetable oil, vegetable oil, and other materials which have melting points in the range of 32–122 °C. In spray chilling, the wall materials have melting points in the range of 32–42 °C, while the wall materials of spray cooling must have melting points in the range of 45–122 °C [26]. The advantage of this process is wall materials with a controlled-release property and the disadvantage is a requirement of special storage conditions [11-12, 27-30].

2.1.3 Freeze drying

Freeze-drying process, which is a freeze dehydration or lyophilization, is suitable for encapsulating thermosensitive ingredients. The freeze-drying steps are quite complicated. First of all, active ingredients and wall materials are dissolved in water. Then, the solution is frozen under low temperatures in the range of -90 to -40 °C. After that, the sample is dried under low pressure, and low temperatures (in the range of

-90 to -20 °C). Finally, this process produces small pieces with pores. However, this process has several disadvantages such as high energy usage, long processing time, and porous products. Therefore, this process is not attractive for various industries [11, 31-35].

2.1.4 Air suspension coating

Air suspension coating (fluid bed coating or spray coating) is a process that is used to encapsulate the active ingredients which are powder or solid particles by coating with coating materials. This process is also widely used in food industries. For the air suspension coating procedure, coating materials are dissolved in the solvent that is easy to evaporate. Then, the solution is sprayed onto the active ingredients that are suspended in a coating chamber by air stream at a specific temperature. The coating materials are deposited on the active ingredients while they are suspended. Finally, the coating materials change from liquid phase to solid film and cover on the surface of active ingredients. The coated active ingredients are moved out from the bottom to the top of the chamber, as shown in Figure 2.2. Even the coating process occurs randomly, the coating film on solid particles of active ingredients is still uniform because the temperature and the humidity of air flow in this process can be controlled. In addition,

the volume of air for fluidization is also controlled because the height of the active ingredients to move freely can be controlled. Air temperature is another important parameter because it produces surface spreading of the coating materials onto the active ingredients. Unsuitable temperature results in incomplete coating of active ingredients.

Viscosity, thermal stability, and film forming ability are the factors used to consider which are suitable coating materials. The coating materials are commonly used in this process, such as cellulose derivatives, dextrans, emulsifiers, lipids, proteins, and starch derivatives. Besides, the hydrogenated vegetable oils or stearines, such as soybean, cottonseed, palm, canola, fatty acids, bee wax, and carnauba wax, are the suitable coating materials for a hot melt coating. However, this process has some disadvantages of a long processing time and a substantial amount of coating materials [36-38].

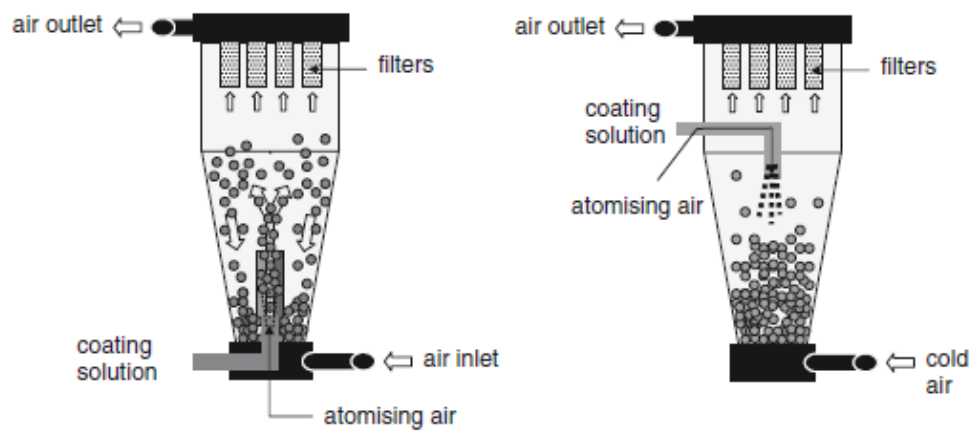


Figure 2.2 Schematic drawing of the air suspension coating process.

2.1.5 Extrusion

Extrusion process is widely used to encapsulate active ingredients, such as flavors, vitamins, and colors. The extrusion process starts with dissolving the active ingredients in a polymer solution. Then, the mixed solution is dropped into a hardening bath by using pipette, syringe, vibrating nozzle, spraying nozzle, jet cutter, coaxial air-flow, electrostatic potential, or atomizing dish. After that, the beads encapsulating the active ingredients are formed. Lastly, the beads are separated from the hardening bath and dried [12, 39-43], as shown in Figure 2.3.

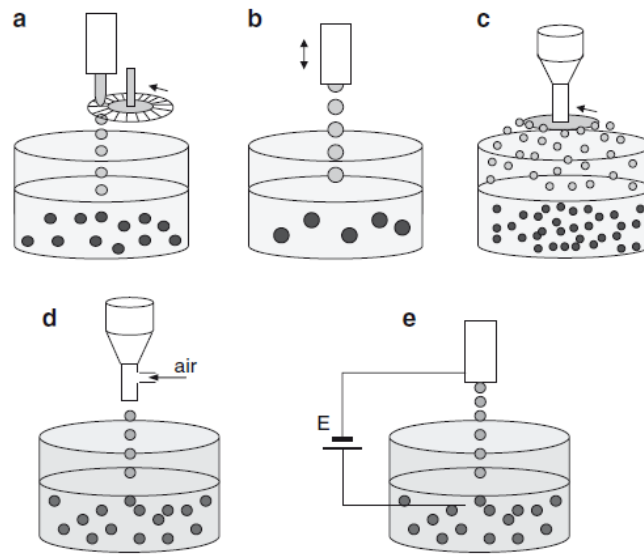


Figure 2.3 Schematic drawing of the extrusion process by dropping the solution by (a) jet-cutter, (b) pipette or vibrating nozzle, (c) atomizing disk, (d) coaxial air-flow, or (e) electrostatic potential into the hardening bath.

2.1.6 Coacervation

Coacervation is a process occurring in colloids. There are two types of processes depending on the type of polymers used in the process. The first type is “simple coacervation” involving only one type of polymers. The other is “complex coacervation”, which uses two or more types of polymers. For a mechanism of simple coacervation process (the encapsulation of citrus oil in gelatin), gelatin was dispersed in water. The citrus oil was added into gelatin solution. Then, this solution was

agitated. The gelatin solution occurs around the citrus oil droplets. After that, the temperature of this solution was reduced to lower than 40 °C because the solubility of gelatin in water is reduced at lowering the temperature causing to form the microcapsules. The limitation of coacervation process is its sensitivity to pH, ionic strength, and temperature [26, 39, 44-47].

2.2 Materials for encapsulation

There are several types of materials used to encapsulate or coat solids, liquids, or gases, depending on their properties and origins. However, materials used in a food industry are stricter than those used in pharmaceutical or cosmetic industries. The materials used in a food industry need a certification for food applications as “generally recognized as safe” (GRAS).

The requirements of materials used for an encapsulation process are to not react with active ingredients, to protect active ingredients from environmental conditions, and to hold active ingredients within beads for a long time. In addition, the cost of the coating materials is also a key factor.

Materials which are extensively used in a food industry for encapsulation are polysaccharides, starch and their derivatives (amylose, amylopectin, dextrans, maltodextrins, polydextrose, syrups, and cellulose

and their derivatives), plant extracts (gum arabic, gum tragacanth, gum karaya, mesquite gum, galactomannans, pectins, and soluble soybean), animal polysaccharides (dextran, chitosan, xanthan, and gellan), marine extracts (carrageenans and alginate), proteins (caseins, gelatine, and gluten), lipid materials (fatty acids and fatty alcohols, waxes (beeswax, carnauba wax, and candellia wax), glycerides, and phospholipids), PVP, paraffin, shellac, and inorganic materials [14, 48].

2.3 Encapsulation of F⁻ in gelatin and ethylcellulose microparticles

Dental caries is a chronic and infectious disease. It occurs from bacteria that generate acids leading to a change in pH within the mouth. A decrease in pH then induces a dissolution of hydroxyapatite in tooth enamel causing the dental caries finally. Nowadays, the dental caries becomes an important public health problem in the world and F⁻ is used for preventing the caries [49-51].

F⁻ is encapsulated in gelatin and ethylcellulose microparticles by spray drying and emulsification with solvent evaporation. Generally, F⁻ in forms of sodium fluoride, sodium monofluorophosphate (MFP), or aminofluoride is used in the encapsulation process. For the preparation of gelatin microparticles using gelatin, F⁻ is dissolved in a gelatin solution.

Then, the mixed solution is spray-dried by a spray dryer. After that, gelatin microparticles are dried and kept in desiccator. For the preparation of ethylcellulose microparticles using ethylcellulose, F^- is dissolved in an ethylcellulose solution. This solution is emulsified by an ultra-disperser, and then solvent is evaporated. Finally, ethylcellulose microparticles were freeze-dried. These processes are easily to encapsulate F^- and they can release in a sustained manner for, at least, 8 hours [52].



CHAPTER III

METHODOLOGY

3.1 Chemicals

Wax-free shellac and calcium chloride (CaCl_2) were purchased from Sigma-Aldrich. Ethanol ($\geq 99.8\%$) was purchased from Merck Ltd., Thailand. Sodium fluoride (NaF) was purchased from Ajax chemical Ltd., Sydney-Melbourne.

3.2 Preparation of shellac bead

A stock solution of 5000-ppm F^- was prepared by dissolving 2.76 g of sodium fluoride (NaF) in 250 mL of deionized (DI) water. To prepare an ethanolic solution of shellac with a shellac concentration of 80 %w/v, 8.00 g of shellac was dissolved in 10 mL of ethanol under a mild stirring for 5 days (shellac-dissolution time). For preparing shellac beads, a solution of 5000-ppm F^- was injected into 10 mL of shellac solutions using a syringe pump with a rate of 500 $\mu\text{L}/\text{minute}$. The NaF droplets in a shellac solution were incubated for 1 minute (bead-formation time) without stirring. Consequently, shellac beads were formed. The formed beads were transferred to DI water, and then further incubated for 2 hours

(bead-hardening time). The beads were dried under an ambient condition.

The schematic process is shown in Figure 3.1.

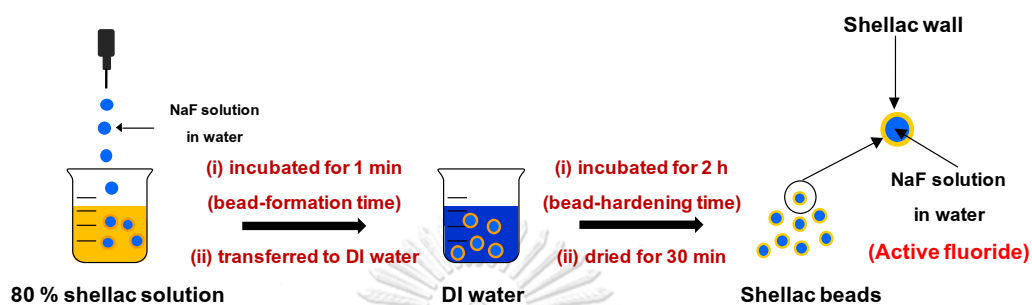


Figure 3.1 Schematic drawing of shellac bead preparation.

3.3 Characterizations

3.3.1 Size and wall thickness of shellac beads

Digital images of shellac beads were collected for determining bead size using an ImageJ software. The thickness of bead wall was analyzed from cross-sectioned shellac bead, which images of bead wall were recorded by a CCD camera (Carl Zeiss, AxioCam HRc) attached on an optical microscope (OM, Carl Zeiss Axio Scope A1).

3.3.2 Morphology and chemical composition

3.3.2.1 Scanning electron microscopy (SEM)

The surfaces of shellac beads were characterized by scanning electron microscope (SEM, JEOL JSM-6510A). A working distance was set at 10 mm. An accelerating voltage was 1 kV using a secondary electron imaging (SEI) mode. For a sample preparation, shellac beads were cross-sectioned by a razor blade, and then washed by DI water. The sample was attached on an aluminum stub using carbon tape and dried under a vacuum condition for 30 minutes before measuring.

3.3.2.2 Energy-dispersive X-ray spectroscopy (EDS)

The chemical compositions of shellac beads were examined using energy-dispersive X-ray spectroscopy (EDS). EDS detector with a liquid nitrogen cooling (JEOL HVB51-X0394) was equipped with SEM (JEOL JSM-6510A). The measurements were operated using a working distance of 10 mm and an acceleration voltage of 20 kV.

3.3.2.3 Fourier-transform infrared (FT-IR) spectroscopy

The functional groups of shellac beads were investigated using Nicolet 6700 FT-IR spectrometer (Thermo Electron Corporation). All FT-

IR spectra were collected by attenuated total reflection (ATR) technique in a single reflection mode with a zinc selenide prism (Harrick, IRK-FTS). The spectral resolution was 4 cm^{-1} and the number of scans was 64 in the spectral range of $4000\text{--}700\text{ cm}^{-1}$.

3.3.3 Crystallinity

The crystallinity of shellac bead was investigated by differential scanning calorimeter (DSC, Mettler Toledo, Stare system DSC 1). Indium was used as a reference and aluminum pan was used as a holder. A heating rate was $10\text{ }^{\circ}\text{C}/\text{minute}$.

3.3.4 Efficiency to store F^{-}

Efficiency of shellac beads to store F^{-} was investigated by immersing a single bead in 10 mL of DI water or 5 % CaCl_2 for different storing times (1–90 days). Then, the bead was rinsed with DI water and transferred to another 10 mL of DI water. After the bead was squeezed, the concentration of F^{-} in DI water was measured by a waterproof fluoride meter (FL700, Extech).

CHAPTER IV

RESULTS AND DISCUSSION

In this chapter, we discuss about the formation mechanism of a shellac bead by using the results from IR spectroscopy. Then, we focus on the optimization for F⁻-encapsulation process of shellac beads by varying several experimental parameters, *i.e.*, shellac concentration, shellac-dissolution time, bead-formation time, and bead-hardening time. Finally, shellac beads before and after F⁻ releasing are characterized to explain an encapsulation mechanism.

4.1 Size and wall thickness of shellac beads

Image of shellac beads and OM image of cross-sectioned shellac bead are presented in Figure 4.1. The average size of F⁻-encapsulated shellac beads is 2.59 ± 0.33 mm counted from 300 beads using a spherical geometry, as shown in Figure 4.1A. Inset also shows a histogram of bead diameters indicating a normal distribution of shellac bead sizes. The wall thickness of bead was analyzed from cross-sectioned shellac beads. The results show that the wall thickness is not uniform due to a gravitational force during the bead-formation step. The thickest and

the thinnest bead walls are 314 ± 82 and 163 ± 31 μm , respectively, as shown in Figure 4.1B. The size of F-encapsulated shellac beads can be controlled by the size of syringe needles in the range of 2.5–10 mm. Unfortunately; the wall thickness cannot be controlled.

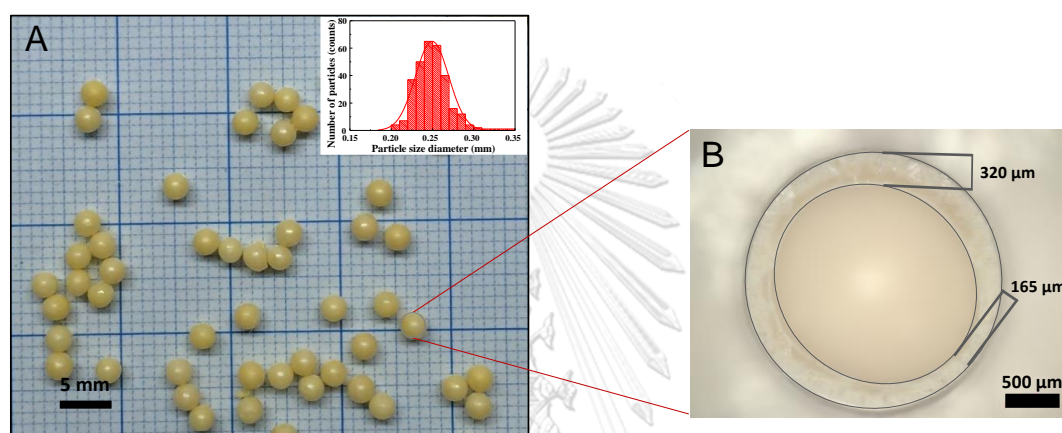


Figure 4.1 (A) F-encapsulated shellac beads prepared from an ethanolic solution of 80 % shellac. Inset shows a histogram of bead diameters. (B) OM image of the cross-sectioned bead showing the thickest and the thinnest walls.

4.2 The formation mechanism of shellac beads

To understand the formation of shellac beads, the formation mechanism of shellac film was firstly investigated by monitoring an

evolution of shellac solution from a liquid phase to a solid film by casting and drying an ethanolic solution of shellac under an ambient condition. Time-dependent IR spectra of shellac during the film formation process are displayed in Figure 4.2. These results give informations about molecular structure changes from a liquid phase to a solid film. From the results, the characteristic peaks of ethanol are at 2969 (C–H stretching), 1085 (C–O stretching), and 1043 cm^{-1} (C–O stretching) [53-54] while the characteristic peaks of shellac are at 2929 (in-phase stretching of $-\text{CH}_2 - \text{CH}_3$), 2853 (out-of-phase stretching of $-\text{CH}_2 - \text{CH}_3$), 1710 (C=O stretching), and 1247 cm^{-1} (O–H bending) [55-56]. At the beginning (0 minute) of the film formation process, the spectrum shows the combination peaks between those of ethanol and shellac. During 30–120 minutes of the process, the peak intensities at 2969, 1085, and 1043 cm^{-1} , which are characteristic peaks of ethanol, decrease with an increase in film formation times. At 120 minutes of the process, the shellac solution completely changes from a liquid phase to a solid film. By comparing the spectrum of shellac before dissolved in ethanol to that of shellac film at 120 minutes of the process, no significant difference can be observed in both spectra, except the characteristic peaks of ethanol. Moreover, by comparing the spectrum of shellac before dissolved in ethanol to that of shellac film kept for 3 days, they are totally superimposed. It implies that

the change from a liquid phase to a solid film occurs from the evaporation of ethanol in the shellac solution with no chemical reaction, as shown in Figure 4.3.

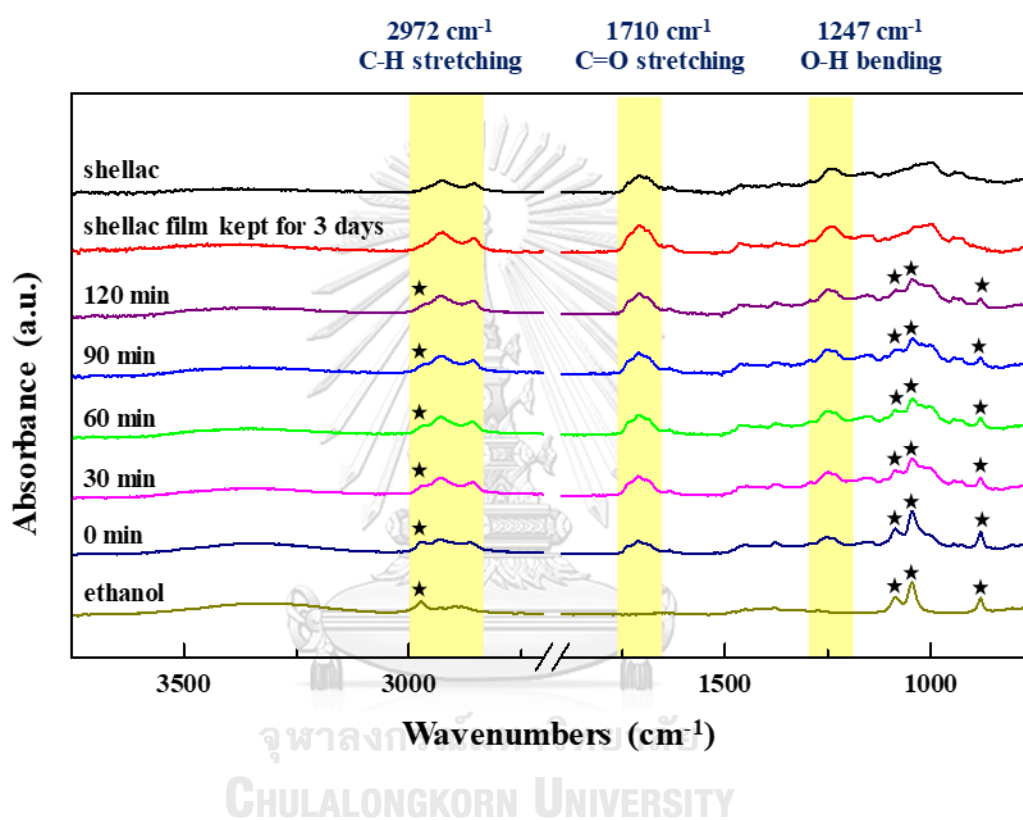


Figure 4.2 Time-dependent IR spectra of shellac film after casting and drying an ethanolic solution of 80 % shellac under an ambient condition.

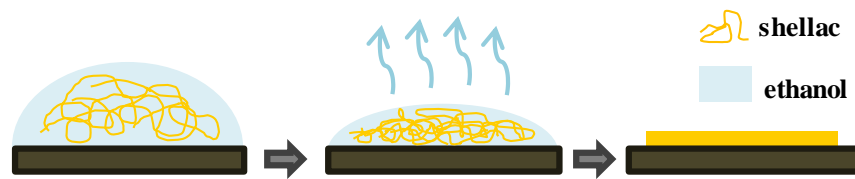


Figure 4.3 The formation of shellac film by an evaporation of ethanol from shellac solution.

Figure 4.4 shows IR spectra of shellac before dissolved in ethanol, shellac film, and shellac bead. These spectra show no significant difference in the main peak of shellac. Therefore, it can be concluded that the process of bead formation is like the process of film formation, which is due to a removal of ethanol in shellac solution.

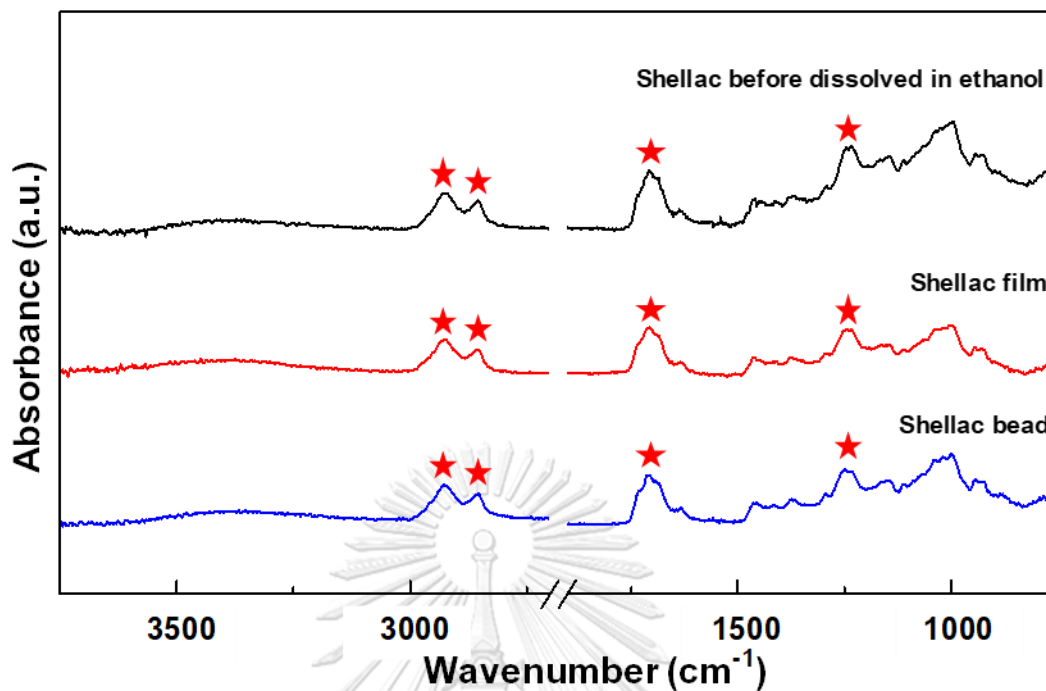


Figure 4.4 IR spectra of shellac before dissolved in ethanol, shellac film, shellac beads.

Similar to the formation of shellac film, the formation mechanism of F⁻-encapsulated shellac bead is depicted in Figure 4.5. Firstly, an aqueous solution of F⁻ is dropped into an ethanolic solution of shellac. Ethanol in the shellac solution diffuses into an aqueous droplet (inside the bead), and then thin-wall shellac bead is formed, which can encapsulate F⁻. This step is a “bead-formation” step. After that, the formed bead is transferred to incubate in DI water. In this step, the wall of shellac bead is

strengthened and hardened by a diffusion of ethanol in a bead wall to an aqueous phase (outside the bead). This step is a “bead-hardening” step.

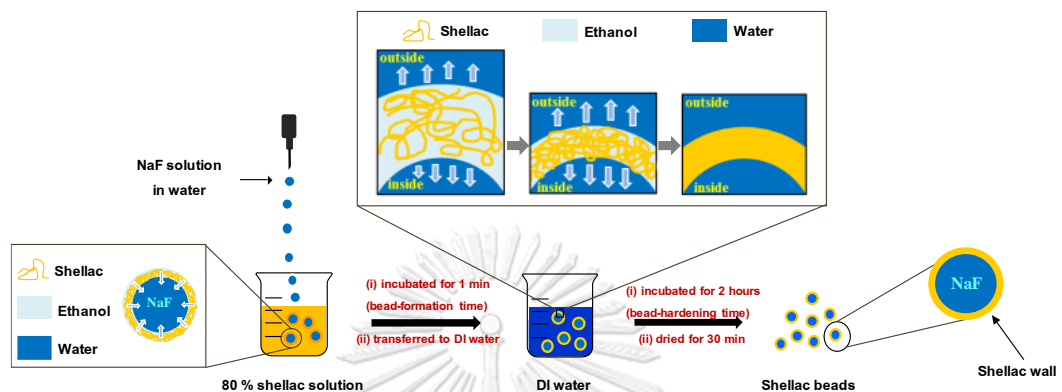


Figure 4.5 The formation of shellac beads by a diffusion of ethanol from shellac solution to aqueous phases.

4.3 Optimization for the preparation of shellac beads

The effects of experimental parameters, *i.e.*, shellac concentration, shellac-dissolution time, bead-formation time, and bead-hardening time, on the formation of shellac beads were elucidated and optimized in this part.

4.3.1 Effect of shellac concentration

Shellac concentration is a crucial parameter for the formation of shellac beads because a viscosity of shellac solution depends directly on the shellac concentration. Figure 4.6 shows percentages of active F^- remaining in shellac beads prepared by various shellac concentrations (60–80 %) after immersed in DI water (1–7 days). Percentages of active F^- in shellac beads after immersed in DI water for 1 day are in the range of 68.00 ± 17.89 to 84.00 ± 4.18 %. The percentages continuously decrease and, after 7 days, the range of percentages is 18.00 ± 5.70 to 27.00 ± 9.08 %. By comparing the percentages of active F^- at the same releasing times, they decrease with an increase in the shellac concentration. The shellac concentration of 80 % is chosen due to the best encapsulation efficiency. For the shellac concentrations of > 80 %, the beads cannot be produced due to a too high viscosity. Moreover, surface morphologies of shellac beads prepared using 70 and 80 % shellac solutions were investigated using SEM.

Figure 4.7 illustrates the effect of shellac concentration on the surface morphologies of shellac beads. The surfaces of both samples show porous morphology. By using 70 % shellac concentration, large pores with a diameter of approximately $5.0 \mu\text{m}$ on a bead surface are observed. When the shellac concentration is increased to 80 %, small pores with a diameter of approximately $0.36 \mu\text{m}$ are observed. This result could be due to higher

viscosity of higher shellac concentration. With a higher viscosity, a diffusion of ethanol in shellac solution to aqueous phases is very slow leading to more uniformity of surface and small pore sizes [57].

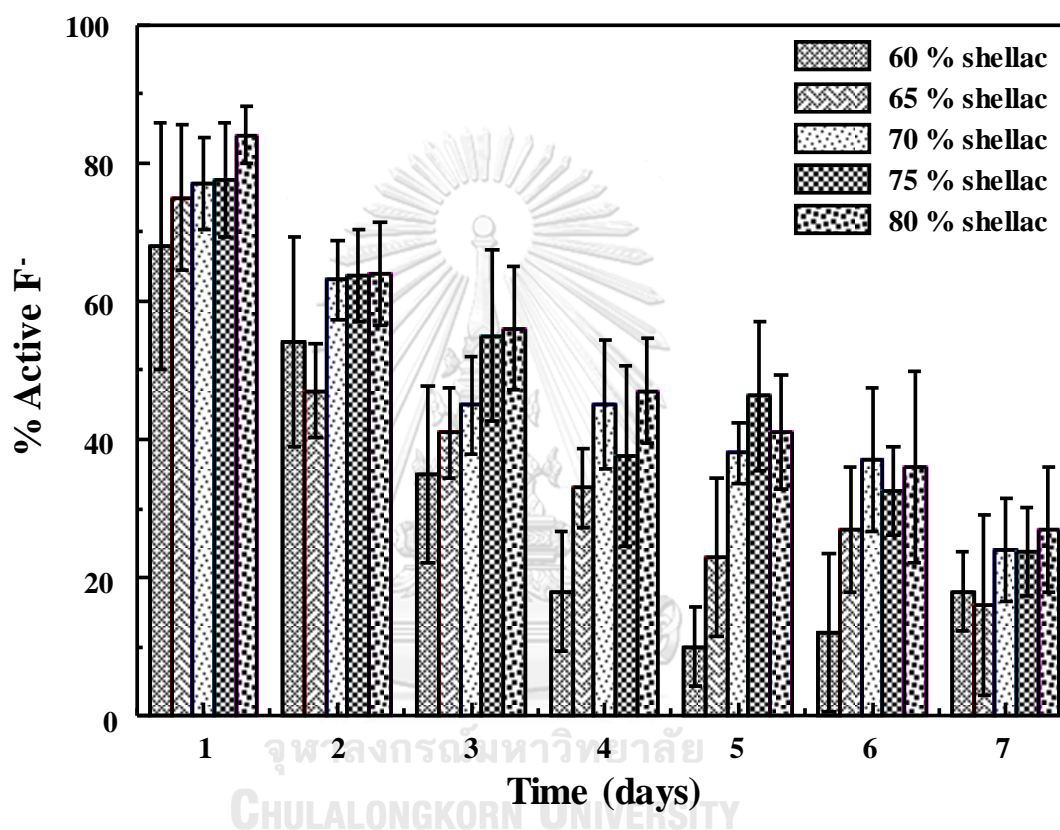


Figure 4.6 Percentages of active F^- remaining in shellac beads prepared by using different shellac concentrations (60–80 %) after immersed in DI water (1–7 days).

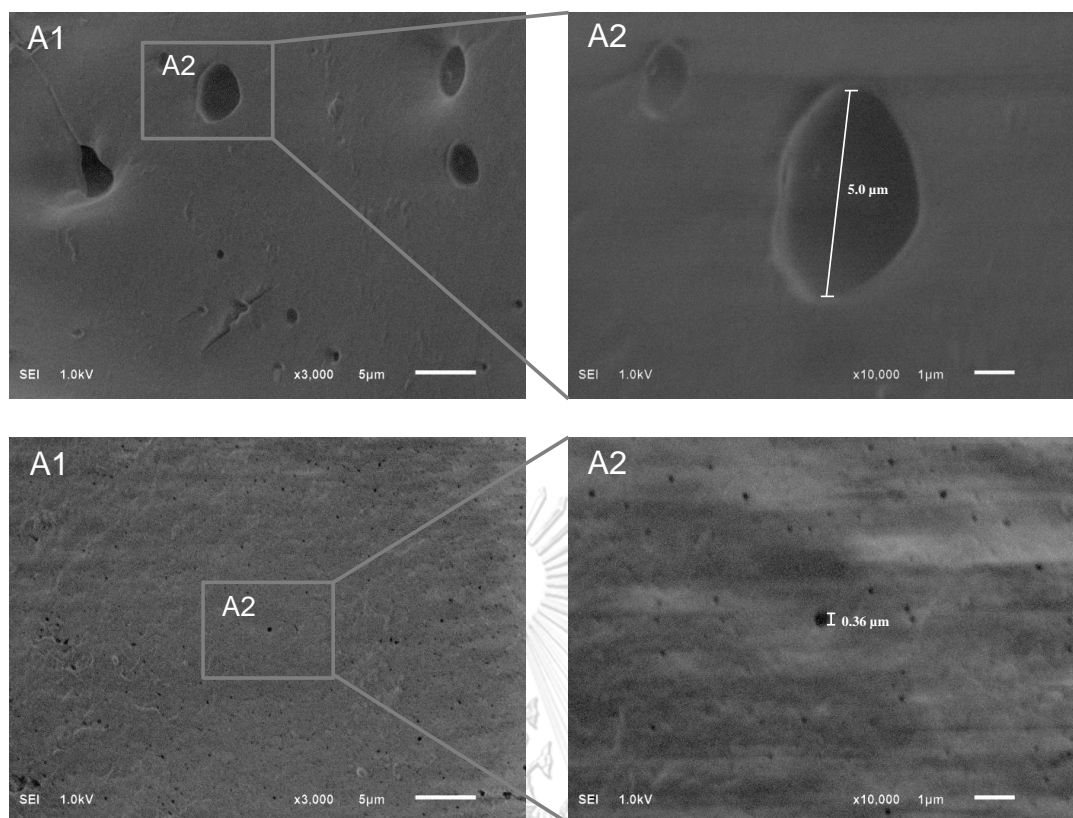


Figure 4.7 SEM images of bead surfaces prepared by using ethanolic solutions of (A) 70 and (B) 80 % shellac.

จุฬาลงกรณ์มหาวิทยาลัย
CHULALONGKORN UNIVERSITY

4.3.2 Effect of shellac-dissolution time

Shellac-dissolution time is another important parameter because, after dissolved in ethanol for long times, polymer chains are swelled and stretched [58], which would alter packing between shellac molecules in the bead. In this section, the shellac-dissolution time was varied from 6 hours to 5 days. Figure 4.8 shows active F^- contents remaining in shellac beads prepared by using various shellac-dissolution times after immersed

in DI water (1–7 days). The results show that percentages of active F^- in the beads decrease with an increase in times of immersion in DI water. After immersed in DI water for 7 days, percentages of active F^- in shellac beads prepared by using the shellac-dissolution times of 6 hours, 1, 2, 3, 4, and 5 days are $27.00 \pm 9.08 \%$, $48.45 \pm 13.76 \%$, 43.88 ± 7.20 , $35.37 \pm 5.55 \%$, $48.17 \pm 7.24 \%$, and $62.07 \pm 9.519 \%$, respectively. It indicates that an increase in shellac-dissolution time prevents a release of F^- from shellac beads. It can be explained that shellac chains are swelled and stretched after dissolved in ethanol. Then, shellac chains are packed closely together to form the bead which reduces leakage of F^- . However, too long shellac-dissolution time is not practically used. Five days of shellac-dissolution time is chosen in this study.

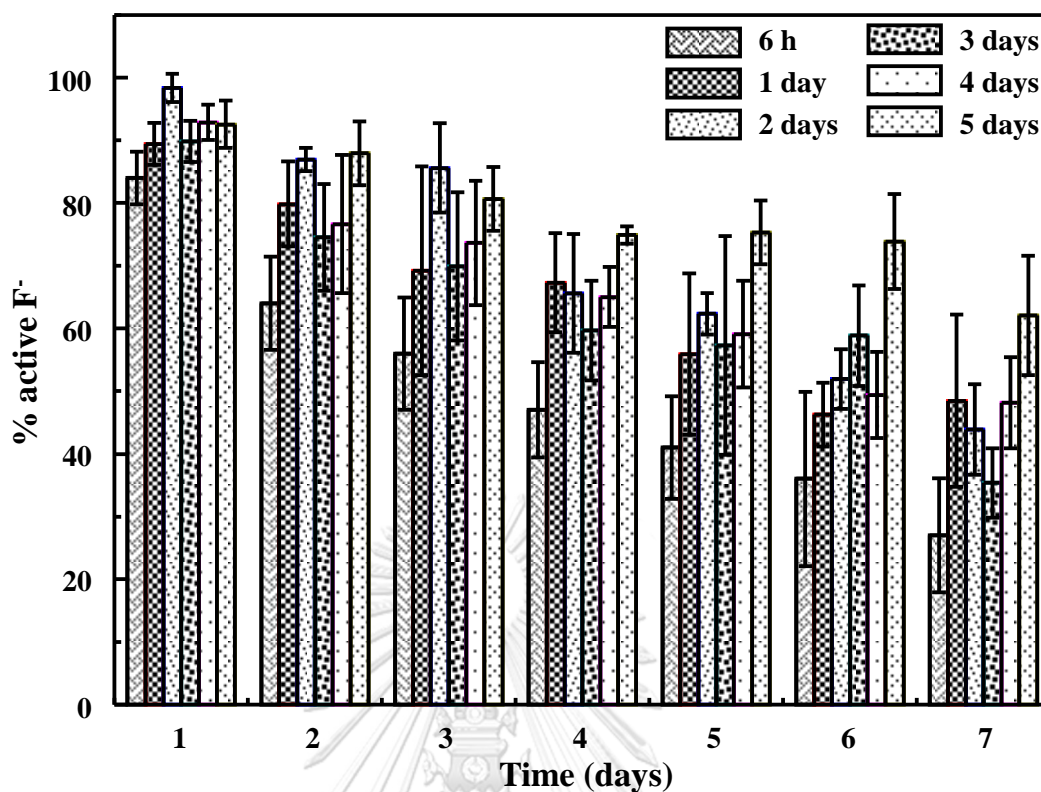


Figure 4.8 Percentages of active F^- remaining in shellac beads prepared by using various shellac-dissolution times after immersed in DI water (1–7 days).

To support an idea about swelling and stretching of polymer chains after dissolving shellac in ethanol. We investigated the viscosity of shellac solution after dissolving shellac in ethanol for 1 day and 5 days. The results show that the viscosity of shellac solution after dissolving shellac in ethanol for 1 day and 5 days are 64.08 and 100.76 poises, respectively.

Therefore, it can imply that shellac in the solution after dissolved for 5 days is swelled and stretched more than that after dissolved for 1 day.

To prove that shellac-dissolution time affects packing between shellac molecules in the beads, crystallinity of the shellac beads was studied using a differential scanning calorimetry (DSC). Figure 4.9 shows DSC profiles of shellac beads with different shellac-dissolution times and shellac before dissolved in ethanol. The results show that DSC thermograms of the shellac before dissolved in ethanol, shellac bead with 1-day shellac-dissolution time, and shellac bead with 5-day shellac-dissolution time show peaks (with onsets) at temperatures of 251.33 (250.03), 169.83 (167.76), 173.50 (172.28) °C, respectively, suggesting that they were molten at different points. It means that the crystallinities of all shellacs are different. DSC thermograms of the shellac beads with 1-day and 5-day dissolution times show a sharp peak implying that shellac chains are rearranged to pack uniformly in the beads. Furthermore, the shellac bead with a 5-day dissolution time shows a sharper peak than that with a 1-day dissolution time indicating more uniformity of shellac chain packing in the bead.

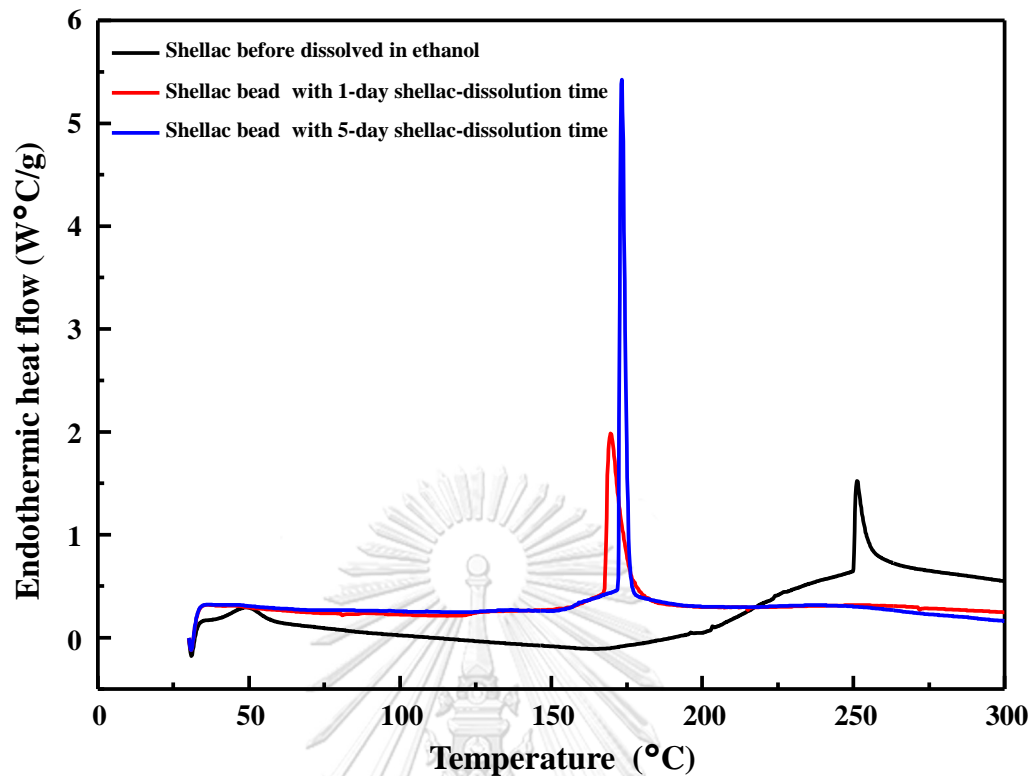
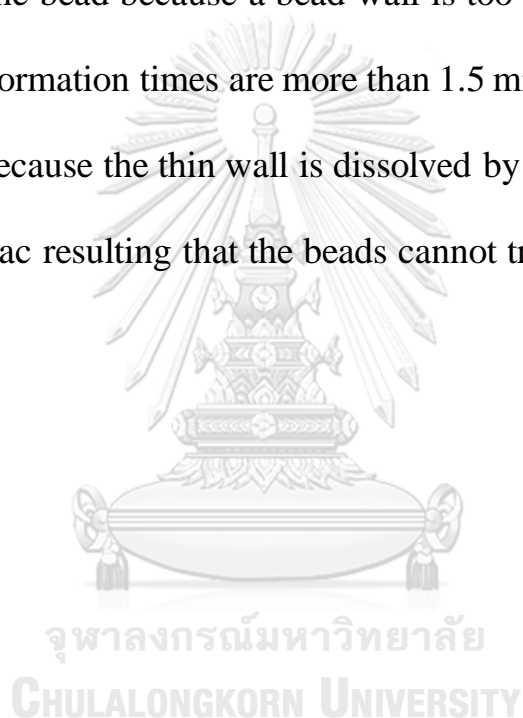


Figure 4.9 DSC thermograms of shellac before dissolved in ethanol and shellac beads prepared by using shellac-dissolution times of 1 and 5 days.

4.3.3 Effect of bead-formation time

Figure 4.10 shows the relation between active F^- remaining in shellac beads and bead-formation time of beads. The results show that percentages of active F^- remaining in shellac beads prepared by using bead-formation times of 0.5, 1.0, and 1.5 minutes after immersed in DI water for

7 days are 48.94 ± 9.29 %, 67.97 ± 6.70 %, and 43.96 ± 13.02 %, respectively. The results do not show a trend. However, the suitable bead-formation time of 1 minute is chosen because it shows the highest percentages of active F^- remaining in shellac beads after immersed in DI water for 7 days. When the bead-formation times are less than 0.5 minute, it cannot form the bead because a bead wall is too thin. In the other hand, when the bead-formation times are more than 1.5 minutes, they also cannot form the bead because the thin wall is dissolved by ethanol in an ethanolic solution of shellac resulting that the beads cannot transferred to DI water.



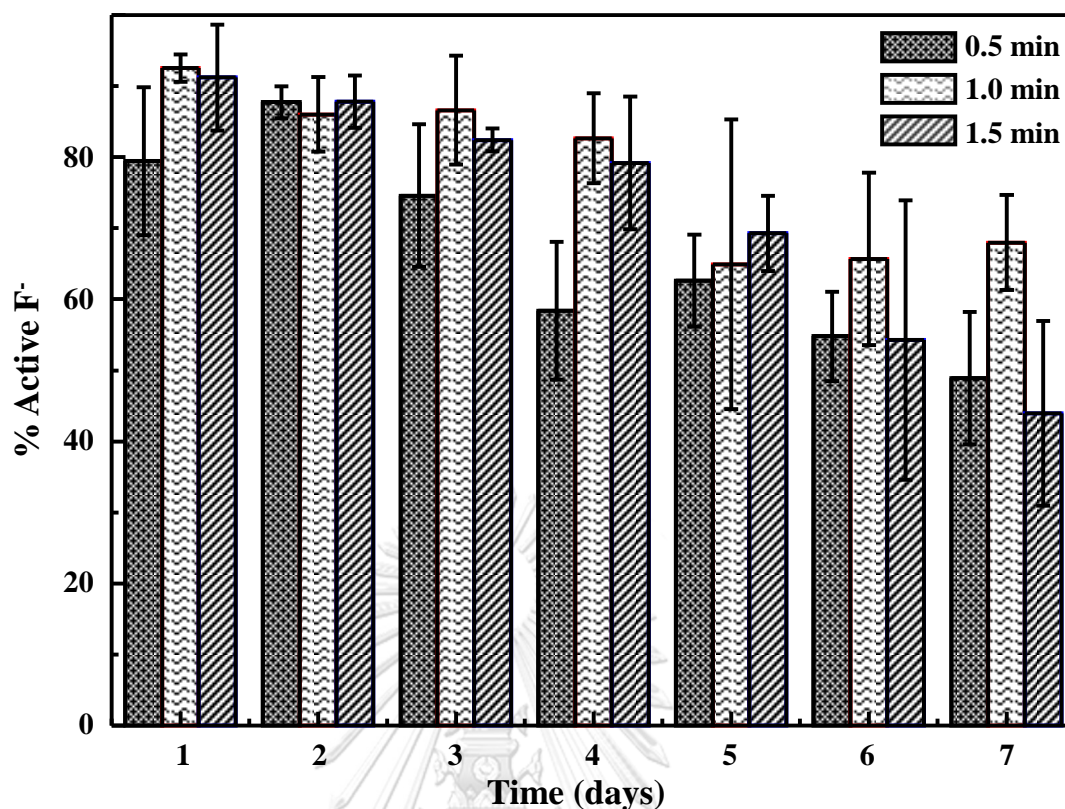


Figure 4.10 Percentages of active F^- remaining in shellac beads prepared by using various bead-formation times after immersed in DI water (1–7 days).

4.3.4 Effect of bead-hardening time

To optimize the bead-hardening time in the preparation process of shellac beads, the bead-hardening time was varied from 0.5 to 5 hours. Figure 4.11 shows the active F^- remaining in shellac beads prepared by using various bead-hardening times. The results show that percentages of the active F^- decrease with an increase in times of immersion. After

immersed in DI water for 7 days, percentages of active F^- in shellac beads prepared by using the bead-hardening times of 0.5, 1, 2, 3, 4, and 5 hours are $48.29 \pm 19.86 \%$, $39.91 \pm 8.04 \%$, $48.39 \pm 19.71 \%$, $46.98 \pm 8.43 \%$, $38.89 \pm 10.31 \%$, $44.70 \pm 12.50 \%$, respectively. The bead-hardening time of 2 hours provides the highest percentages of active F^- remaining in shellac beads after immersed in DI water for 7 days. Hence, the bead-hardening time of 2 hours is suitable and chosen in this work.



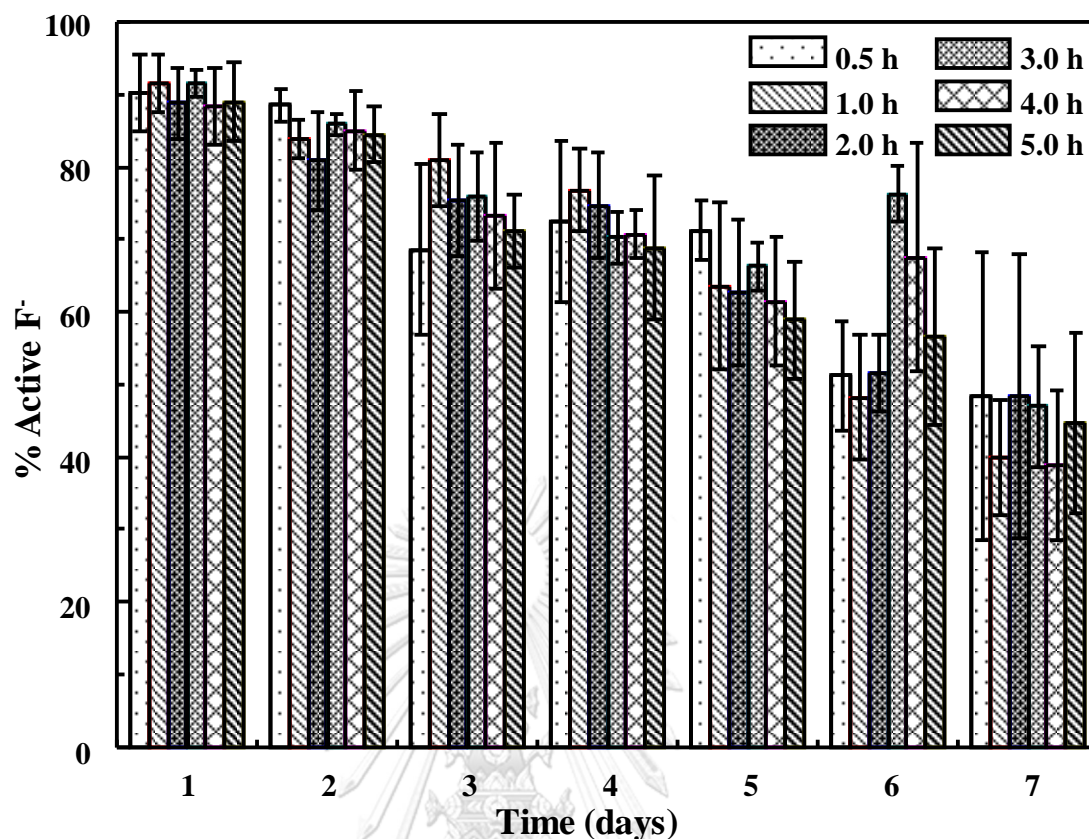
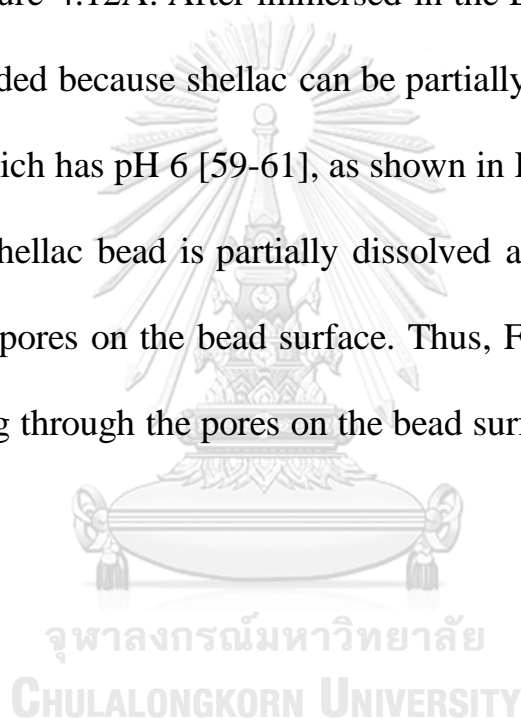


Figure 4.11 Percentages of active F⁻ remaining in shellac beads prepared by using various bead-hardening times after immersed in DI water (1–7 days).

After optimizing the conditions for the preparation of shellac bead to achieve the best encapsulation efficiency of active F⁻, we found that the optimal condition is 80 % shellac concentration, shellac-dissolution time of 5 days, bead-formation time of 1 minute, and bead-hardening time of

2 hours. This condition gives the active F^- of 48.39 ± 19.71 % remaining in shellac beads after immersed in DI water for 7 days.

Next, the morphologies of bead surfaces before and after immersed in DI water for 7 days were studied using SEM. The results suggest that, before immersed in DI water, the bead surface contains several small pores, as shown in Figure 4.12A. After immersed in the DI water for 7 days, the pores are expanded because shellac can be partially dissolved and swelled in a solution which has pH 6 [59-61], as shown in Figure 4.12B. As pH of DI water is 6, shellac bead is partially dissolved and swelled resulting in enlargement of pores on the bead surface. Thus, F^- can be released to DI water by passing through the pores on the bead surface.



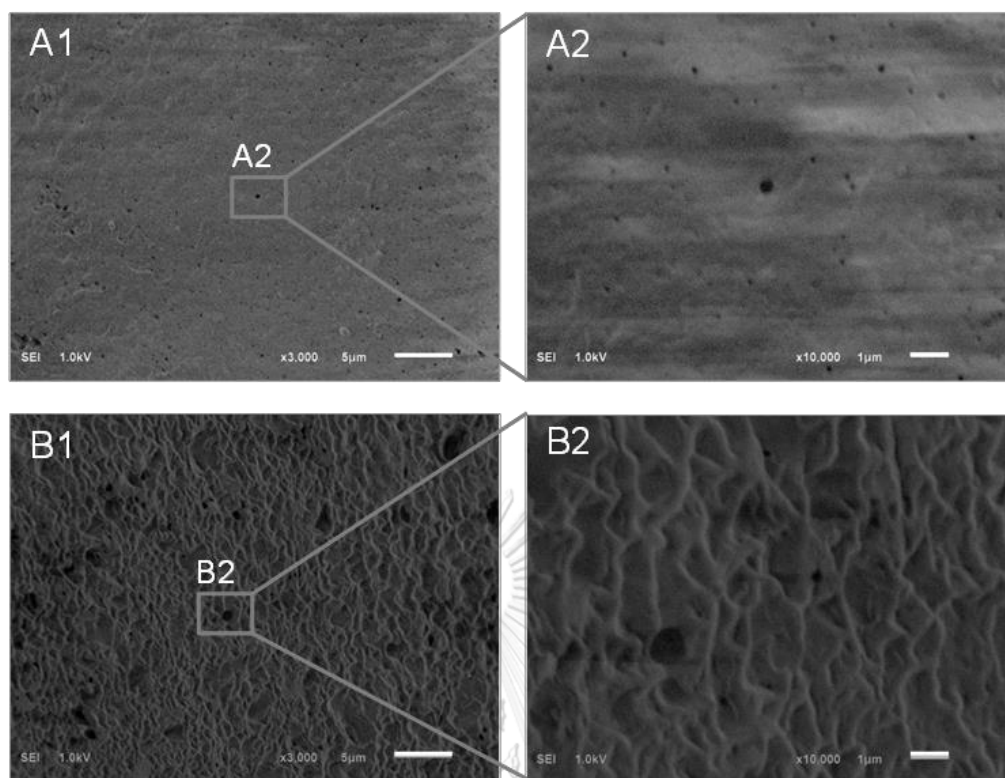


Figure 4.12 SEM images of bead surfaces (A) before and (B) after immersed in DI water for 7 days.

The chemical functional groups of shellac beads before and after immersed in DI water for 7 days were investigated by IR spectroscopy. Their IR spectra are presented in Figure 4.13. From the results, there is no significant difference in both spectra. It can be concluded that no chemical functional group changes during a process of F^- release.

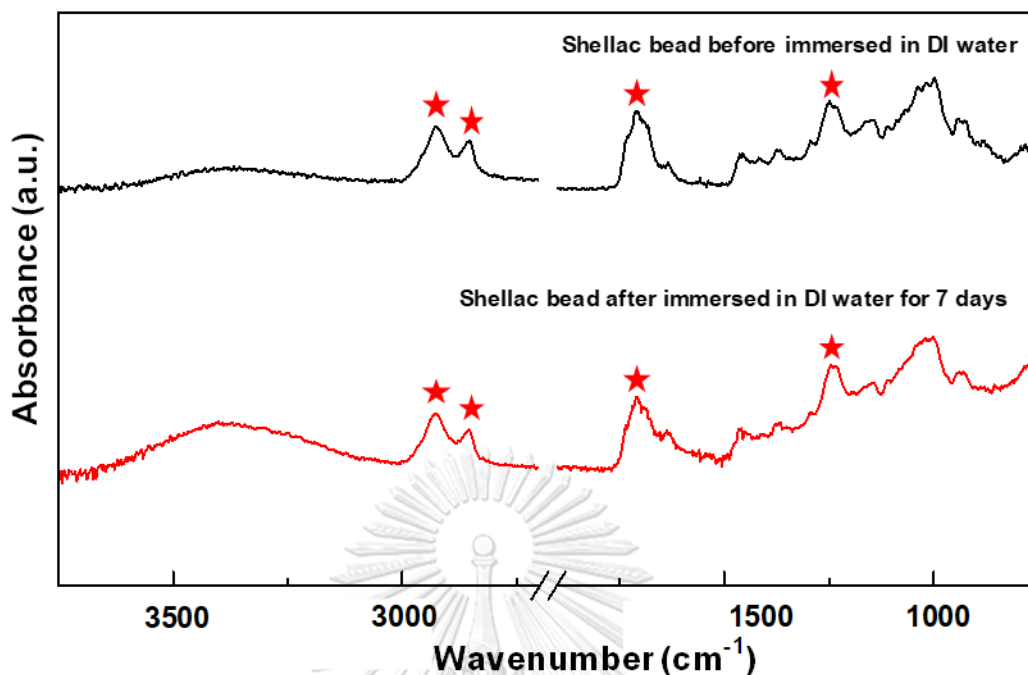


Figure 4.13 IR spectra of bead surfaces (A) before and (B) after immersed in DI water for 7 days.

4.4 F^- encapsulation in 5 % CaCl_2 solution

To monitor F^- encapsulation of shellac beads in a calcium matrix, shellac beads were immersed in 5 % CaCl_2 for 1–90 days and the concentrations of active F^- remaining in the beads were determined. Figure 4.14 shows percentages of active F^- remaining in shellac beads after immersed in 5 % CaCl_2 for 1–14 days. Percentages of active F^- are quite constant in the range of 70.87 ± 5.11 % to 82.00 ± 5.46 %.

On the other hand, percentages of active F^- decrease continuously when immersed in DI water and it completely depletes after immersed for 14 days.

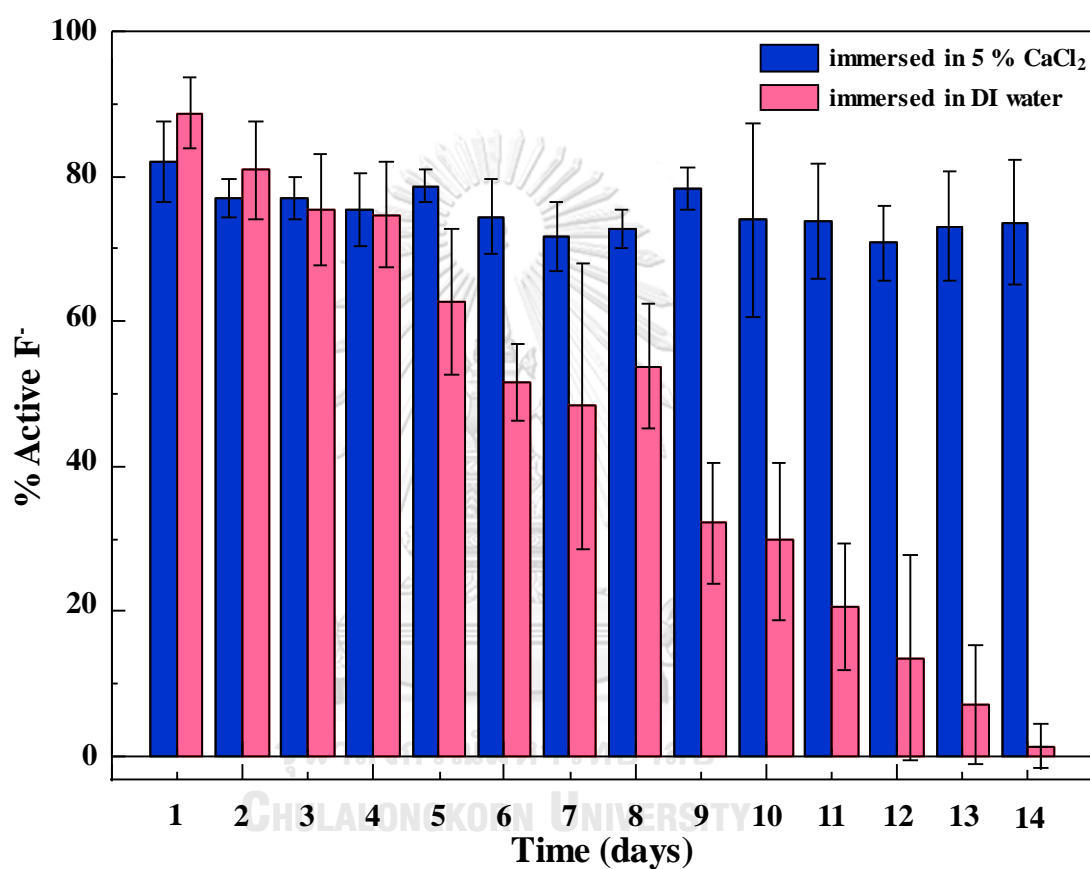


Figure 4.14 Percentages of active F^- remaining in shellac beads after immersed in DI water and 5 % $CaCl_2$ for 1–14 days.

Figure 4.15 shows percentages of active F^- remaining in shellac beads after immersed in 5 % $CaCl_2$ for 1–90 days. Percentages of active F^-

are still quite constant in the range of 67.78 ± 6.31 % to 82.00 ± 5.46 %. After 90 days of immersion, the percentage of active F^- remaining in the beads is still 71.03 ± 4.18 %. It suggests that this shellac beads can encapsulate the active F^- for, at lease, 90 days or 3 months.

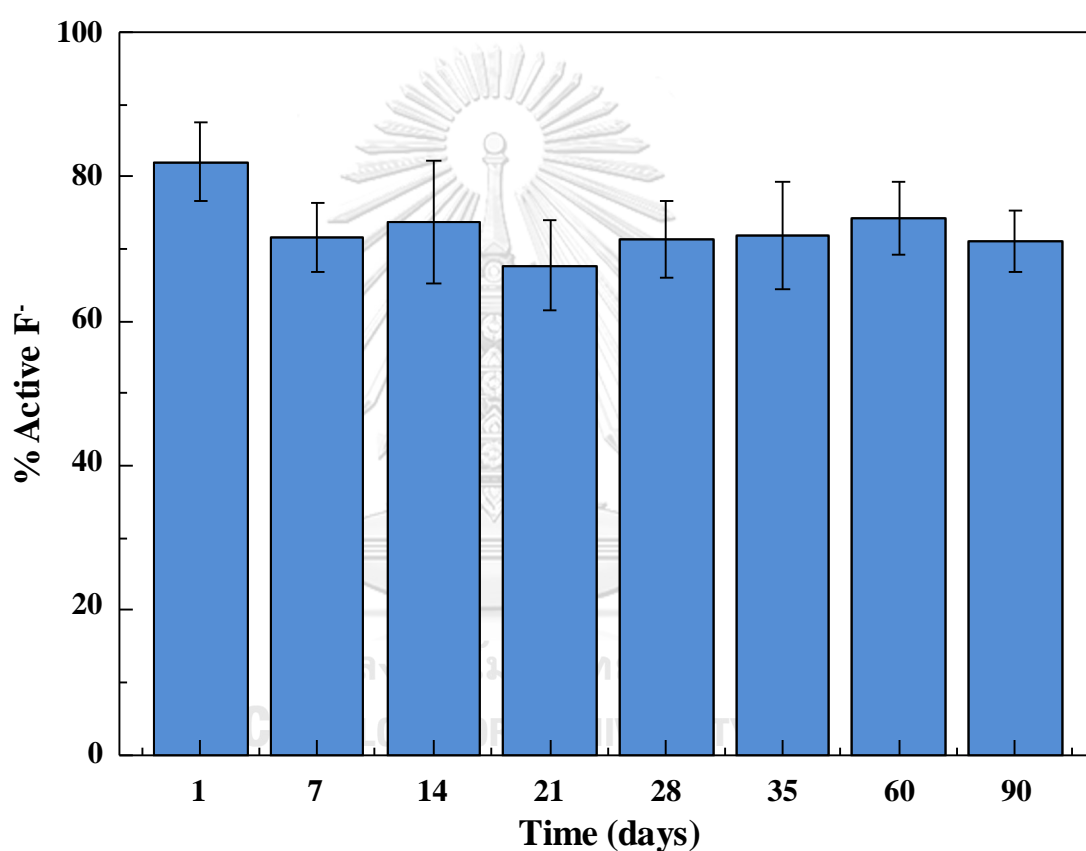
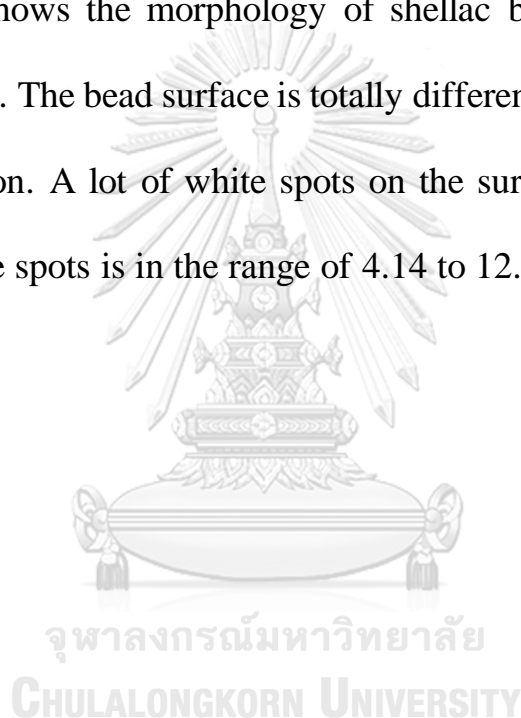


Figure 4.15 Percentages of active F^- remaining in shellac beads after immersed in 5 % $CaCl_2$ for 1–90 days.

4.5 Morphology of shellac beads in 5 % CaCl₂

The morphologies of bead surfaces before and after immersed in 5 % CaCl₂ for 7 days were investigated using SEM. The bead surface before immersed in a CaCl₂ solution contains several small pores with the size of approximately 0.36 μm , as shown in Figure 4.16A. Figure 4.16B shows the morphology of shellac bead after immersed in a CaCl₂ solution. The bead surface is totally different from the bead surface before immersion. A lot of white spots on the surface are observed. The size of the white spots is in the range of 4.14 to 12.25 μm .



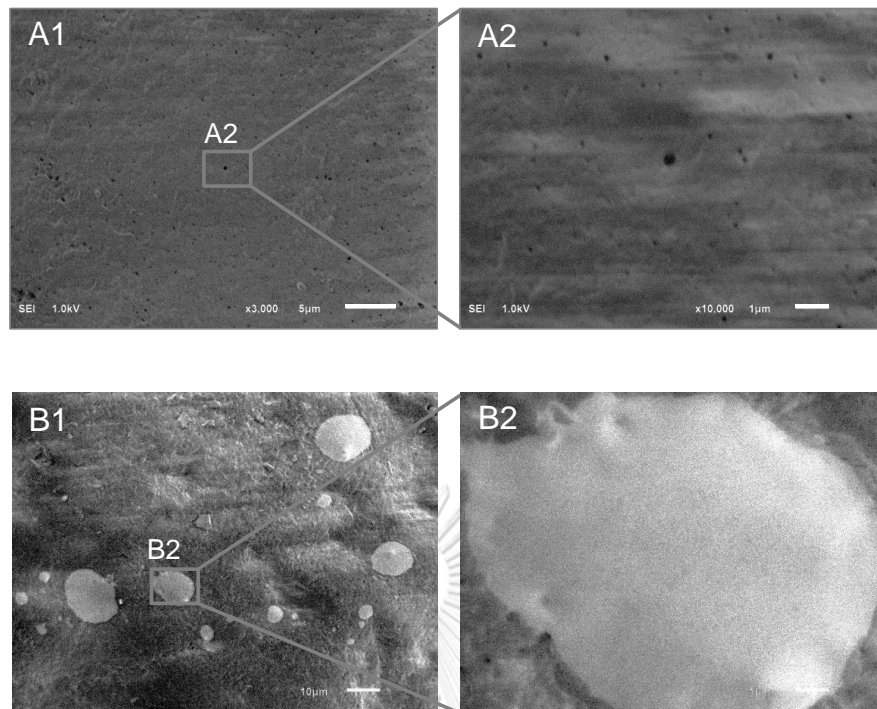


Figure 4.16 SEM images of bead surfaces (A) before and (B) after immersed in 5 % CaCl_2 for 7 days.

The white spots would be CaF_2 because they are insoluble in water [62]. To confirm that, the elemental compositions of white spots on the bead surface were investigated using EDS technique. Figure 4.17A–E shows the elemental maps (carbon, oxygen, fluoride, and calcium) representing the distribution of atoms on the bead surface. The results show that carbon and oxygen distributed in the bead surface, but they are not found in the areas of white spots. On the other hand, fluoride and calcium are found in white spot areas, but they are not found at other positions.

Figure 4.17F shows an EDS spectrum collected from the (×) position in Figure 4.17A. The results show that fluoride and calcium are found with % atoms of 1.98 and 0.82 %, respectively. A ratio of % atoms between fluoride and calcium is also approximately 2 : 1. These results strongly confirm that the white spots on the surface bead are CaF_2 .

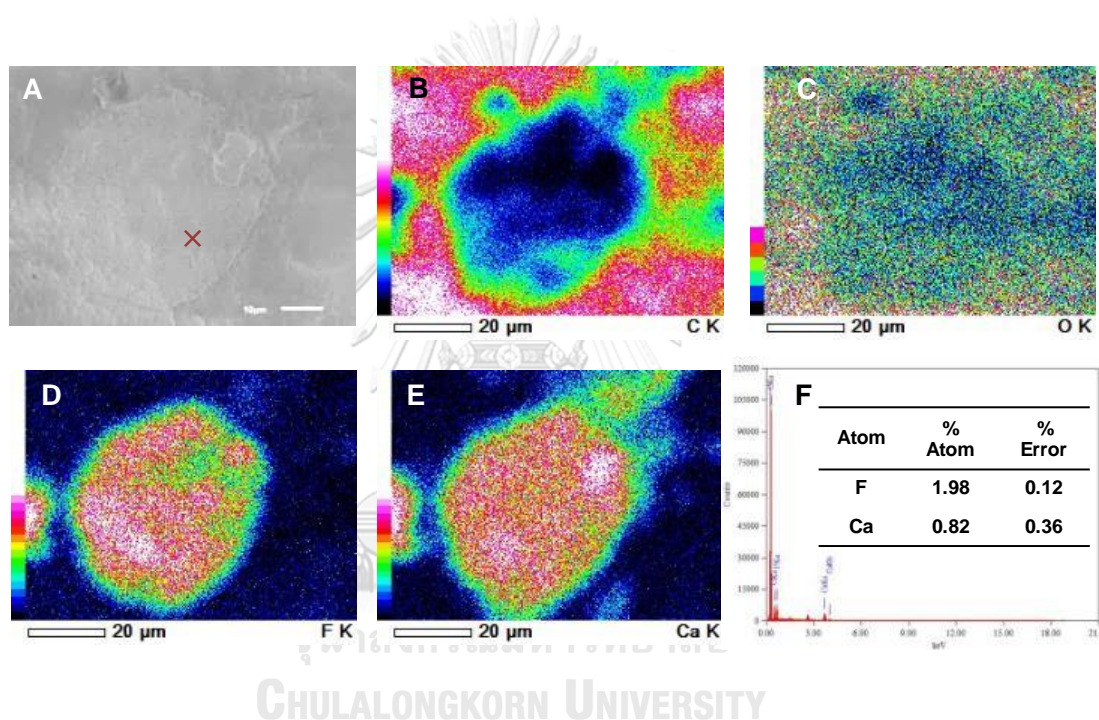


Figure 4.17 (A) SEM image and elemental maps of (B) carbon, (C) oxygen, (D) fluoride, and (E) calcium collected from the surface of shellac bead after immersed in 5 % CaCl_2 for 7 days, (F) EDS spectrum collected from the (×) position in Figure 4.17A.

4.6 The proposed mechanism of CaF₂ formation on the bead surface

A cross-sectioned shellac bead after immersed in a CaCl₂ solution was also characterized using EDS technique, as shown in Figure 4.18. The results show elemental maps of carbon, oxygen, fluoride, and calcium comparing to the original SEM image. Figures 4.18D–E present the distributions of fluoride and calcium in the bead wall, which indicate a pathway of CaF₂ formation inside a channel of the pore. It suggests the formation mechanism of CaF₂ on the bead surface. Figure 4.19 presents the proposed mechanism of the CaF₂ formation on the bead surface after immersed in 5 % CaCl₂. The active F⁻ inside shellac beads goes through the channel of pore on the bead surface. Meanwhile, Ca²⁺ outside the bead goes into the bead thru the pores. Once active F⁻ meets Ca²⁺ in the channel, they react each other and CaF₂ is formed. Therefore, CaF₂ can block the releasing channel of active F⁻ resulting that the bead can encapsulate the active F⁻ for, at least, 3 months with the encapsulation efficiency of 71.03 ± 4.18 %.

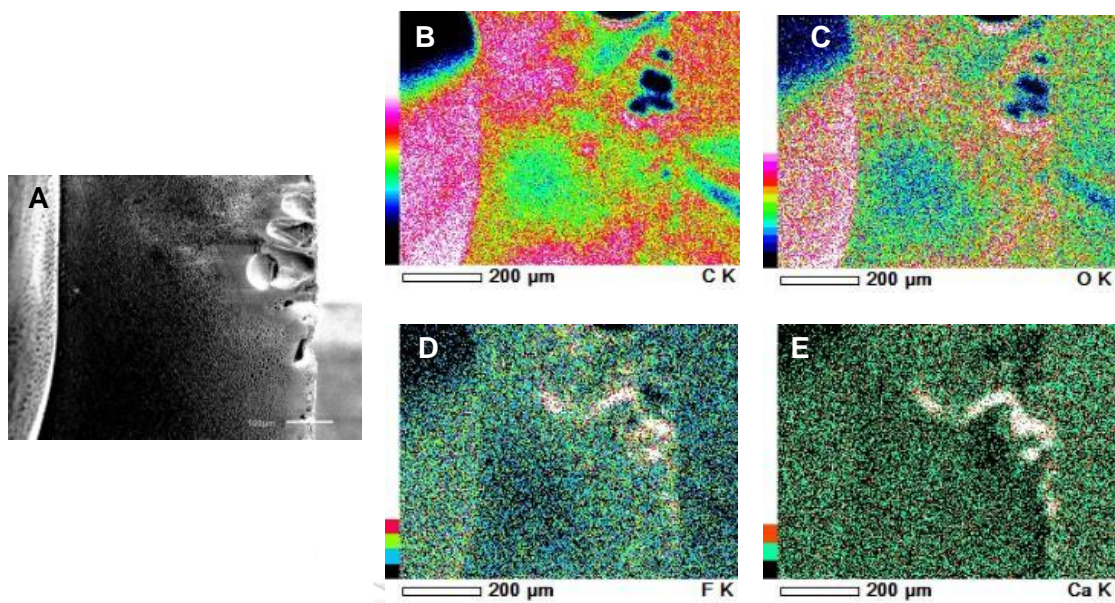


Figure 4.18 (A) SEM image and elemental maps of (B) carbon, (C) oxygen, (D) fluoride, and (E) calcium collected from the shellac bead wall after immersed in 5 % CaCl_2 for 7 days.

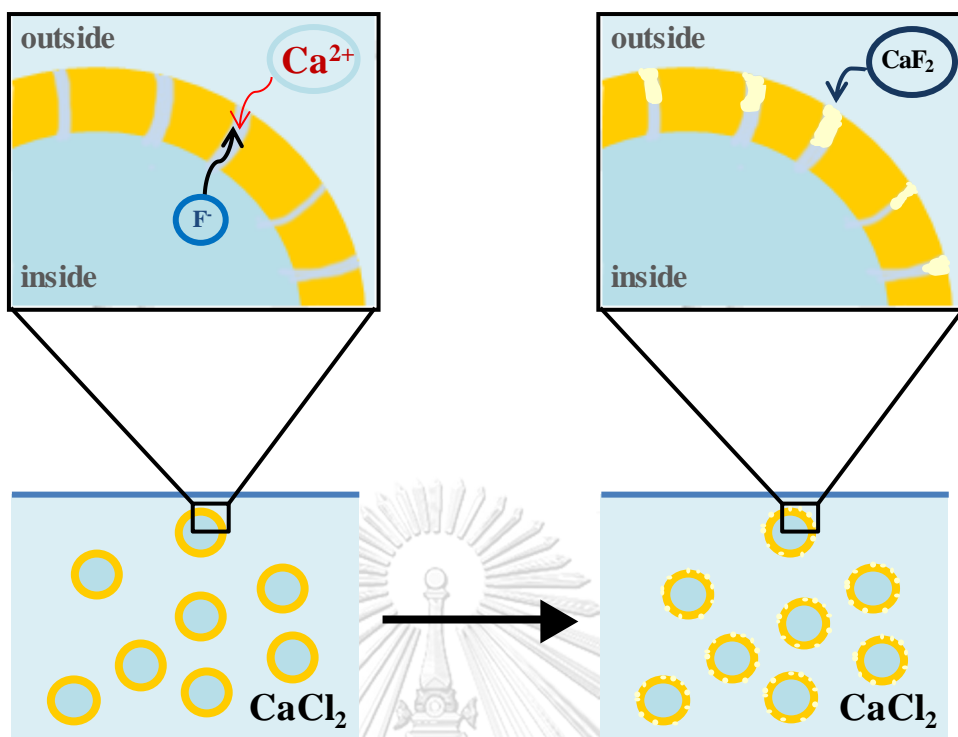


Figure 4.19 The proposed mechanism of the CaF_2 formation on the bead surface.

CHAPTER V

CONCLUSIONS

5.1 Conclusions

According to our designed and developed protocol, F⁻ was encapsulated in shellac beads by a simple extrusion method. F⁻-encapsulated shellac beads are formed by injecting an aqueous solution of F⁻ into an ethanolic solution of shellac using a syringe pump. After that, the formed shellac beads were transferred to DI water for hardening a bead wall. The mechanism of bead formation was confirmed by IR spectroscopy. From the results, the beads were formed due to a diffusion of ethanol in the bead wall to aqueous phases. The average size of shellac beads was 2.59 ± 0.33 mm. The wall thickness was not uniform due to a gravitational force during the bead-formation step. The thickest and the thinnest bead walls were 314 ± 82 and 163 ± 31 μm , respectively. To obtain the best encapsulation efficiency of active F⁻ in shellac bead, the optimal condition of bead formation was 80 % shellac concentration, shellac-dissolution time of 5 days, bead-formation time of 1 minute, and bead-hardening time of 2 hours. This condition provided the highest efficiency of F⁻ encapsulation after immersed shellac beads in DI water for

7 days, which was 48.39 ± 19.71 % of active F^- remaining in the beads. Unfortunately, active F^- completely released after immersed in DI water for 14 days. However, after immersed in 5 % $CaCl_2$ for 14 days, percentages of active F^- remaining in the beads were slightly fluctuate in the range of 70.87 ± 5.11 % to 82.00 ± 5.46 %. Moreover, F^- was still in the beads after immersed in 5 % $CaCl_2$ for 90 days with the percentage of 71.03 ± 4.18 %. This long encapsulation time comes from the formation of CaF_2 which blocks releasing channels of F^- on the bead surface. From these results, this research greatly provides a potential application in oral care industries.

5.2 Suggestions

The size of shellac bead is still too big for applying in a toothpaste application. Further experiments are needed to minimize the size of the polymer bead down to approximately 500 micrometers by using a microfluidic method.

REFERENCES

1. Featherstone, J. D. B., The science and practice of caries prevention. *Journal of the American Dental Association*, **2000**. *131* (7), 887-899.
2. Featherstone, J. D. B., Prevention and reversal of dental caries: role of low level fluoride. *Community Dentistry and Oral Epidemiology*, **1999**. *27* (1), 31-40.
3. Hamilton, I. R., Biochemical effects of fluoride on oral bacteria. *Journal of Dental Research*, **1990**. *69*, 660-667.
4. Loveren, C. V., The antimicrobial action of fluoride and its role in caries inhibition. *Journal of Dental Research*, **1990**. *69*, 676-681.
5. Cate, J. M. t.; Featherstone, J. D. B., Mechanistic aspects of the interactions between fluoride and dental enamel. *Critical Reviews in Oral Biology and Medicine*, **1991**. *2* (3), 283-296.
6. Featherstone, J. D. B.; Glena, R.; Shariati, M.; Shields, C. P., Dependence of in vitro demineralization of apatite and remineralization of dental enamel on fluoride concentration. *Journal of Dental Research*, **1990**. *69*, 620-625.

7. West, N.; Seong, J.; Macdonald, E.; He, T.; Barker, M.; Hooper, S., A randomised clinical study to measure the anti-erosion benefits of a stannous-containing sodium fluoride dentifrice. *Journal of Indian Society of Periodontology*, **2015**. *19* (2), 182-187.
8. Kidd, O. F. a. E., *Dental caries: the disease and its clinical management*. second edition, 2009, Markono Print Media Pte Ltd, Singapore.
9. Wason, S. K., *High fluoride compatibility dentifrice abrasives and compositions*. 1982, U.S. Patent.
10. Augustin, M. A.; Hemar, Y., Nano- and micro-structured assemblies for encapsulation of food ingredients. *Chemical Society Reviews*, **2009**. *38* (4), 902-912.
11. Desai, K. G. H.; Jin Park, H., Recent developments in microencapsulation of food ingredients. *Drying Technology*, **2005**. *23* (7), 1361-1394.
12. Gouin, S., Microencapsulation: industrial appraisal of existing technologies and trends. *Trends in Food Science and Technology*, **2004**. *15* (7), 330-347.

13. Madene, A.; Jacquot, M.; Scher, J.; Desobry, S., Flavour encapsulation and controlled release – a review. *International Journal of Food Science and Technology*, **2006**. *41* (1), 1-21.
14. Nedovic, V.; Kalusevic, A.; Manojlovic, V.; Levic, S.; Bugarski, B., An overview of encapsulation technologies for food applications. *Procedia Food Science*, **2011**. *1*, 1806-1815.
15. Tari, T. A.; Singhal, R. S., Starch based spherical aggregates: reconfirmation of the role of amylose on the stability of a model flavouring compound, vanillin. *Carbohydrate Polymers*, **2002**. *50* (3), 279-282.
16. Limmatvapirat, S.; Limmatvapirat, C.; Puttipipatkachorn, S.; Nuntanid, J.; Luangtana-anan, M., Enhanced enteric properties and stability of shellac films through composite salts formation. *European Journal of Pharmaceutics and Biopharmaceutics*, **2007**. *67* (3), 690-698.
17. Limmatvapirat, S.; Nunthanid, J.; Puttipipatkachorn, S.; Luangtana-anan, M., Effect of alkali treatment on properties of native shellac and stability of hydrolyzed shellac. *Pharmaceutical Development and Technology*, **2005**. *10* (1), 41-46.

18. Luangtana-anan, M.; Limmatvapirat, S.; Nunthanid, J.; Wanawongthai, C.; Chalongsuk, R.; Puttipipatkachorn, S., Effect of salts and plasticizers on stability of shellac film. *Journal of Agricultural and Food Chemistry*, **2007**. *55* (3), 687-692.
19. Luangtana-anan, M.; Nunthanid, J.; Limmatvapirat, S., Effect of molecular weight and concentration of polyethylene glycol on physicochemical properties and stability of shellac film. *Journal of Agricultural and Food Chemistry*, **2010**. *58* (24), 12934-12940.
20. Qussi, B.; Suess, W. G., Investigation of the effect of various shellac coating compositions containing different water-soluble polymers on in vitro drug release. *Drug Development and Industrial Pharmacy*, **2005**. *31* (1), 99-108.
21. Wang, J.; Chen, L.; He, Y., Preparation of environmental friendly coatings based on natural shellac modified by diamine and its applications for copper protection. *Progress in Organic Coatings*, **2008**. *62* (3), 307-312.
22. Xue, J.; Zhang, Z., Preparation and characterization of calcium-shellac spheres as a carrier of carbamide peroxide. *Journal of Microencapsulation*, **2008**. *25* (8), 523-530.

23. Gharsallaoui, A.; Roudaut, G.; Chambin, O.; Voilley, A.; Saurel, R., Applications of spray-drying in microencapsulation of food ingredients: An overview. *Food Research International*, **2007**. *40* (9), 1107-1121.
24. F. Gibbs, S. K. I. A. C. N. M. B., Encapsulation in the food industry: a review. *International Journal of Food Sciences and Nutrition*, **1999**. *50* (3), 213-224.
25. Watanabe, Y.; Fang, X.; Minemoto, Y.; Adachi, S.; Matsuno, R., Suppressive effect of saturated acyl l-ascorbate on the oxidation of linoleic acid encapsulated with maltodextrin or gum arabic by spray-drying. *Journal of Agricultural and Food Chemistry*, **2002**. *50* (14), 3984-3987.
26. Risch, S. J.; Reineccius, G. A., Encapsulation and controlled release of food ingredients. *American Chemical Society*, **1995**. *590*, 103-109.
27. Risch, S. J., Review of patents for encapsulation and controlled release of food ingredients. in encapsulation and controlled release of food ingredients, *American Chemical Society*, **1995**. *590*, 196-203.
28. Shahidi, F.; Han, X. Q., Encapsulation of food ingredients. *Critical Reviews in Food Science and Nutrition*, **1993**. *33* (6), 501-547.

29. Jafari, S. M.; Assadpoor, E.; He, Y.; Bhandari, B., Encapsulation efficiency of food flavours and oils during spray drying. *Drying Technology*, **2008**. 26 (7), 816-835.
30. Augustin, M.; Sanguansri, L.; Margetts, C.; Young, B., Microencapsulating food ingredients. *Food Australia*, **2001**. 53 (6), 220-223.
31. Desobry, S. A.; Netto, F. M.; Labuza, T. P., Comparison of spray-drying, drum-drying and freeze-drying for β -carotene encapsulation and preservation. *Journal of Food Science*, **1997**. 62 (6), 1158-1162.
32. Fang, Z.; Bhandari, B., Encapsulation of polyphenols – a review. *Trends in Food Science and Technology*, **2010**. 21 (10), 510-523.
33. Kharaghani, A.; Tsotsas, E.; Wolf, C.; Beutler, T.; Guttzeit, M.; Oetjen, G.-W., *Ullmann's Encyclopedia of Industrial Chemistry* 2000, Wiley-VCH Verlag GmbH and Co. KGaA, Germany.
34. Munin, A.; Edwards-Lévy, F., Encapsulation of natural polyphenolic compounds; a review. *Pharmaceutics*, **2011**. 3 (4), 793-829.

35. Laine, P.; Kylli, P.; Heinonen, M.; Jouppila, K., Storage stability of microencapsulated cloudberry (*rubus chamaemorus*) phenolics. *Journal of Agricultural and Food Chemistry*, **2008**. *56* (23), 11251-11261.
36. Dewettinck, K.; Huyghebaert, A., Fluidized bed coating in food technology. *Trends in Food Science and Technology*, **1999**. *10* (4), 163-168.
37. Guichard, E., Flavour retention and release from protein solutions. *Biotechnology Advances*, **2006**. *24* (2), 226-229.
38. Guignon, B.; Duquenoy, A.; Dumoulin, E. D., Fluid bed encapsulation of particles: principles and practice. *Drying Technology*, **2002**, *20* (2), 419-447.
39. Strauss, G.; Gibson, S. M., Plant phenolics as cross-linkers of gelatin gels and gelatin-based coacervates for use as food ingredients. *Food Hydrocolloids*, **2004**. *18* (1), 81-89.
40. Zuidam, N. J.; Shimoni, E., Overview of Microencapsulates for Use in Food Products or Processes and Methods to Make Them. In *Encapsulation Technologies for Active Food Ingredients and Food*. Springer New York. 2010. 3-29.
41. Risch, S. J.; Reineccius, G. A., Flavor encapsulation. *American Chemical Society*, **1988**. 370, 220.

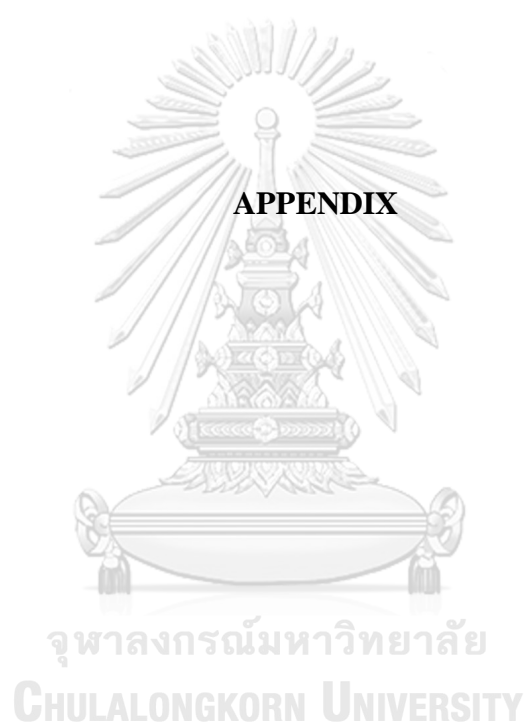
42. Madene, A.; Jacquot, M.; Scher, J.; Desobry, S., Flavour encapsulation and controlled release—a review. *International journal of food science and technology*, **2006**. *41* (1), 1-21.
43. Uhlemann, J.; Schleifenbaum, B.; BERTRAM, H.-J., Flavor encapsulation technologies: an overview including recent developments. *Perfumer and flavorist*, **2002**. *27* (5), 52-61.
44. Kruif, de C. G.; Weinbreck, F.; Vries, de R., Complex coacervation of proteins and anionic polysaccharides. *Current Opinion in Colloid and Interface Science*, **2004**. *9* (5), 340-349.
45. Lemetter, C. Y. G.; Meeuse, F. M.; Zuidam, N. J., Control of the morphology and the size of complex coacervate microcapsules during scale-up. *AIChE J*, **2009**, *55* (6), 1487-1496.
46. Soper, J. C., Utilization of coacervated flavors. in encapsulation and controlled release of food ingredients, *American Chemical Society*, **1995**. *590*, 104-112.
47. Alvim, I. D.; Grosso, C. R. F., Microparticles obtained by complex coacervation: influence of the type of reticulation and the drying process on the release of the core material. *Food Science and Technology (Campinas)*, **2010**. *30* (4), 1069-1076.

48. Zuidam, N. J.; Nedovic, V., Encapsulation technologies for active food ingredients and food processing. *Springer New York*, **2009**. 31–100.
49. Hicks, J.; Garcia-Godoy, F.; Flaitz, C., Biological factors in dental caries: role of remineralization and fluoride in the dynamic process of demineralization and remineralization (part 3). *Journal of Clinical Pediatric Dentistry*, 2004. 28 (3), 203-214.
50. Keegan, G. M.; Smart, J. D.; Ingram, M. J.; Barnes, L.-M.; Burnett, G. R.; Rees, G. D., Chitosan microparticles for the controlled delivery of fluoride. *Journal of Dentistry*, 2012. 40 (3), 229-240.
51. Diarra, M.; Pourroy, G.; Boymond, C.; Muster, D., Fluoride controlled release tablets for intrabuccal use. *Biomaterials*, 2003. 24 (7), 1293-1300.
52. de Francisco, L. M. B.; Cerquetani, J. A.; Bruschi, M. L., Development and characterization of gelatin and ethylcellulose microparticles designed as platforms to delivery fluoride. *Drug Development and Industrial Pharmacy*, 2013. 39 (11), 1644-1650.
53. Greenler, R. G., Infrared study of the adsorption of methanol and ethanol on aluminum oxide. *Journal of Chemical Physics*, **1962**. 37 (9), 2094-2100.

54. Plyler, E. K., Infrared spectra of methanol, ethanol, and n-propanol. *Journal of Research of the National Bureau of Standards*, **1952**. 48 (4), 281-286.
55. P.C., S.; A.K., S., FTIR spectroscopy of lac resin and its derivatives. *Pigment and Resin Technology*, **1997**. 26 (6), 378-381.
56. P.C., S.; K.K., K., An investigation into the different forms of lac resin using FT-IR and diffuse reflectance spectroscopy. *Pigment and Resin Technology*, **2001**. 30 (1), 25-34.
57. Strawhecker, K. E.; Kumar, S. K.; Douglas, J. F.; Karim, A., The critical role of solvent evaporation on the roughness of spin-cast polymer films. *Macromolecules*, **2001**. 34 (14), 4669-4672.
58. Miller-Chou, B. A.; Koenig, J. L., A review of polymer dissolution. *Progress in Polymer Science*, **2003**. 28 (8), 1223-1270.
59. Buch, K.; Penning, M.; Wächtersbach, E.; Maskos, M.; Langguth, P., Investigation of various shellac grades: additional analysis for identity. *Drug Development and Industrial Pharmacy*, **2009**. 35 (6), 694-703.
60. Farag, Y.; Leopold, C. S., Development of shellac-coated sustained release pellet formulations. *European Journal of Pharmaceutical Sciences*, **2011**. 42 (4), 400-405.

61. Farag, Y.; Leopold, C., Physicochemical properties of various shellac types. *Dissolution Technology*, **2009**. *16*, 33-39.
62. Patnaik, P., *Handbook of inorganic chemicals*. 2003, McGraw-Hill, New York.





Conference Presentations:

1. Fluoride encapsulation under calcium (Ca^{2+}) ion matrix (poster presentation), The 3rd International Congress on Advanced Materials (AM 2016), 27–30 November 2016, Centara Grand at Central Plaza Ladprao, Bangkok, Thailand
2. Fluoride encapsulation using edible polymer (oral presentation), The 43rd Congress on Science and Technology of Thailand (STT 43), 17–19 October 2017, Chamchuri 10, Chulalongkorn University, Bangkok, Thailand

Scholarship and Awards:**2016**

Award: The second prize of the 9th Science and Technology Initiative and Sustainability Awards (STISA) in concept of “Creative Processes and Materials for Social Sustainability”, 1 August 2016

Organized by: Thai Institute of Chemical Engineering and Applied Chemistry cooperated with Dow Chemical Company and SCG Chemical Company

Invention: Unique silver jewelry from industrial and chemical laboratory wastes

2017

Award: The second prize of Invention and Innovation Contest of Graduate Students 2016 (proposal), 23-26 August 2017

Organized by: National Research Council of Thailand (NRCT)

Invention: Silver dust: a ready to use silver nanoparticle Powder



VITA

Name: Miss Piyada Dissara

Address: 25 Village No. 6, Sathing Mo, Singha Nakhon, Songkhla
90280, Thailand

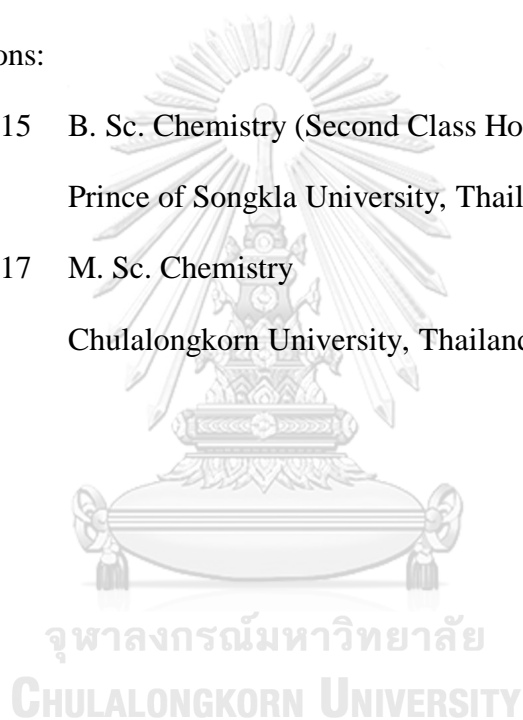
E-mail: piyada_1630@hotmail.com Tel: (+66)87-4795844

Personal: Born 16 February 1992, Songkhla, Thailand

Educations:

2011-2015 B. Sc. Chemistry (Second Class Honors)
Prince of Songkla University, Thailand

2015-2017 M. Sc. Chemistry
Chulalongkorn University, Thailand





จุฬาลงกรณ์มหาวิทยาลัย
CHULALONGKORN UNIVERSITY